Eva Pump

Olefin Metathesis with *cis*-Dichloro Ruthenium Benzylidene Complexes: *New Mechanistic Insights*

Master Thesis

Diplomarbeit

zur Erlangung des akademischen Grades eines
Diplom -Ingenieurs

der Studienrichtung Technische Chemie
erreicht an der Technischen Universität Graz

Jänner 2011

Betreuer: Univ.-Doz. Dipl. Ing. Dr. techn. Christian Slugovc
Institut für Chemische Technologie und Materialien
Technische Universität Graz

Acknowledgement

I am most grateful to all those who supported me and helped me to complete this work:

I thank Christian Slugovc for supervising my thesis, for his motivation, the helpful discussions and for the opportunity of participating at international conferences.

My gratitude goes to Michaela Zirngast, who started working on this issue, for sharing data and her versatile know-how with me. I want to thank Anita Leitgeb for supervising me and her contagious enthusiasm and all my colleagues at the ICTM for their helpfulness and the interesting discussions about chemical and non chemical topics inside and outside from university

I would like to thank Petra Kaschnitz for NMR measurements, Josephine Hobisch for GPC measurements and Jörg Albering for X-ray crystal structures.

Financial support by the EUMET project is gratefully acknowledged

In the end I would like to express my gratitude to my parents for their financial and mental support and their faith in me. Further I want to thank the rest of my family and all of my friends for accompanying me for all the years.

Abstract

In the last years more and more latent *cis*-dichloro ruthenium initiators for olefin metathesis and especially for ring opening metathesis polymerization (ROMP) have been disclosed and characterized. In this contribution novel initiators, prepared from the precursor complex (H_2IMes)(py)$(Cl)_2$Ru(3-phenyl-*1H*-inden-1-ylidene) and a chelating ligand (various 4-methoxy-2-vinyl-benzoic acid ester derivatives) are presented. Special attention is paid to a side product occurring in the synthesis of the *iso*-propyl dichloro complex that was determined to be a cationic pyridine containing analogue to the main product. Most interestingly, this complex revealed higher catalytic activity in ROMP polymerization than the dichloro compound. Detailed investigations of the cationic species and a related derivative by means of NMR spectroscopy and X-ray diffraction (XRD) as well as GPC analysis of the polymers brought new insights in the mechanistic behavior of *cis*-dichloro initiators. It is suggested, that the aforementioned cationic pyridine adduct is an intermediate during the isomerization of the rather latent *cis* dichloro complex to its more active *trans*-dichloro isomer.

Kurzfassung

In den letzten Jahren wurden immer mehr latente *cis*-Dichloro Ruthenium Initiatoren für Olefin Metathese und speziell für Ring öffnende Metathese Polymerisation (ROMP) charakterisiert und veröffentlicht. In diesem Zusammenhang werden neue Verbindungen vorgestellt, die aus dem Precursor-Komplex (H_2IMes)(py)$(Cl)_2$Ru(3-phenyl-*1H*-inden-1-yliden) und einem chelatisierenden Liganden (verschiedene 4-Methoxy-2-vinyl-benzoesäureester Derivate) hergestellt wurden. Ein besonderes Augenmerk galt einem Nebenprodukt, welches in der Herstellung von dem Dichloro-isopropyl Komplex gefunden wurde und sich als analoger, kationischer Komplex mit einem koordinierenden Pyridin herausstellte. Genauere Untersuchung von der kationischen Spezies und einem verwandten Derivat mit Hilfe von NMR Spektroskopie und Röntgenbeugung (XRD), sowie GPC Analysen der Polymere brachten neue Einblicke in das mechanistische Verhalten von *cis*-Dichloro Initiatoren. Es wurde vorgeschlagen, dass das vorher angeführte kationische Pyridin-Addukt als Zwischenprodukt während der Isomerisierung von dem ziemlich latenten *cis*-Dichloro Komplex auftritt und zu der viel aktiveren *trans* Dichloro Verbindung isomerisiert.

Table of Content

1. Introduction

1.1. *cis*-Dichloro Ruthenium Complexes

Since the discovery of the first well-defined, metathesis-active ruthenium alkylidene complexes[1] in 1992, they became indispensible for initiating metathesis reactions. Many works have aimed on improving stability, reactivity, activity and the functional group tolerance,[2] thus, a variety of commercially available catalysts with a *trans* stereochemistry of the two halide ligands emerged. The first striking observations, regarding isomers of the conventional *trans*-dichloro ruthenium complexes with *cis* stereochemistry of the two halides occurred in 1993, when Grubbs et al. carried out derivatizations on first generation Grubbs complexes.[3] It remained not clear, if the *cis*-isomers exist as stable, non-interconverting species, until Hansen et al. isolated the first Grubbs-type metathesis catalyst with a fixed cis-stereochemistry of the chloride ligands.[4] Although these complexes have similar steric and electronic properties, compared to well-known, *trans*-dichloro compounds, their catalytical metathesis activity was not that high, attributed to a lower initiation rate. However, this property is beneficial in ring opening metathesis polymerization (ROMP), meaning a longer handling of the monomer-catalyst mixture, before polymerization starts. For that reason, further works have been aimed on synthesis[5] and thermodynamic behavior[6] of this kind of catalysts.

---

[1] Nguyen, S. T.; Johnson, L. K.; Grubbs, R. H. *J. Am. Chem. Soc.*. **1992**, 114, 3974-3975

[2] Sanford, M. S.; Love, J. A.; Grubbs, R. H. *Organometallics* **2001**, 20, 531

[3] Nguyen, S. T.; Grubbs, R. H. *Inorg. Chem.* **1993**, 115, 9858-9859

[4] Hansen, S. M; Rominger, F.; Metz, M.; Hofmann, P. *Chem. Eur. J.* **1999**, 5, No. 2, 557-566

[5] Diesendruck, C. E.; Tzur, E; Ben-Asuly, A.; Goldberg, I.; Straub, B. F.; Lemcoff, N. G. *Inorg. Chem.* **2009**, 48, 10819-10825

[6] Poater, A., Ragone, F., Correa, A., Szadkowska, A., Barbasiewicz, M, Grela, K., Cavallo, L., *Chem. Eur. J.* **2010**, DOI: 20010.1002/chem.201001849

1.2. Scope of this Work

The objective of this work was the preparation and characterization of new *cis*-dichloro ruthenium complexes bearing chelating ligands, namely 4-methoxy-2-vinyl-benzoic acid ester derivatives. Further, the new ruthenium complexes should be tested in ring opening metathesis polymerization (ROMP) to find a trend between the catalytic activity and the influence of the ester residue.

Due to the unforeseen appearance of a cationic, pyridine containing complex in the synthesis of a *cis*-dichloro compound, the focus was shifted towards this species. The newfound initiator and a related derivative were characterized using different methods as ^{1}H NMR, ^{13}C NMR and single crystal X-ray diffractometry and benchmarked in typical ROMP reactions. The obtained results allow a proposal of new mechanistic impacts regarding the entrance of *cis*-dichloro complexes into the catalytic cycle of olefin metathesis.

2. General Background

2.1. From ill-Defined Ruthenium Halide-Based Complexes to *cis*-Dichloro Ruthenium Initiators

It was a long path until a good understanding for preparing well defined ruthenium based olefin metathesis catalysts had been created. On the one hand it was known, that ruthenium was an excellent candidate due to its functional group tolerance, but on the other hand the understanding of how to achieve this high functional group tolerance was limited, so ruthenium based complexes had not been considered for many years.[7]

The first ill-defined initiators, such as $RuCl_3$(hydrate), that were active in ring opening metathesis polymerization (ROMP) for high strained olefins, appeared in the 1960s.[8] Nevertheless, it took three decades until the benefits of these late transition metal complexes were immensely enhanced by the introduction of neutral ligands and alkylidenes, yielding well-defined L_2X_2Ru=CHR type complexes (**I**, L = PCy_3, X = Cl, Grubbs "1st generation").[9]

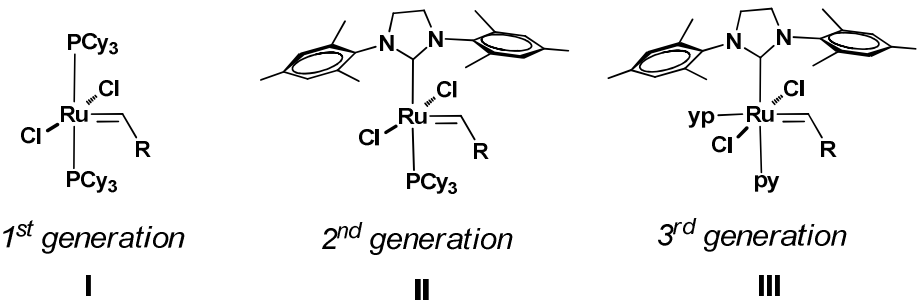

Figure 1. Modification of well defined ruthenium alkylidene complexes leaded to higher activity and better initiation rates

---

[7] Trnka, M. T.; Grubbs, R. H. *Acc. Chem. Res.* **2001**, 34, 18-29

[8] Rinehart, R. E.; Smith, H. P. *Polymer Letters* **1965**, Vol. 3, 1049-1052

[9] *Handbook of Metathesis*, ed. Grubbs, R. H. Wiley-VCH, Weinheim 2003

Subsequently, it became necessary, to modify the complexes in order to improve stability, reactivity, activity and the functional group tolerance (see Figure 1). In the so called **II**, "2nd generation" catalysts , the trialkylphosphine ligand was exchanged for an N-heterocyclic carbene (NHC) moiety,[10,11] leading to not only an improvement in selectivity for binding olefin substrates instead of free phosphine , but also a great boost in reactivity.[12] These tendencies can be explained by the electronic properties of the NHC moiety, providing excellent donor properties relative to trialkylphosphine.[13] Another performance-enhancing modification concerned the replacement of the second phosphine ligand by pyridine and led to so-called "3rd generation" initiators like **III**,[14] which shows excellent activity in ROMP.[15]

Compared to great efforts dealing with above outlined improvements of the metathesis catalyst's performance, much less studies have been aimed at systematically decreasing the initiation rate of well defined ruthenium complexes. A lower initiation rate can be of advantage in ring opening metathesis polymerization (ROMP), regarding the possibility of a longer handling of the monomer/catalyst mixture, before the polymerization starts.[16] One of the first ruthenium systems featuring a lower catalytic activity and yet a better stability compared to first generation complexes **I** (depicted in Figure 1) occurred in 1999, when Hoveyda et al. proposed the formation of a Ru-chelate complex by a ligand exchange procedure, starting from $L_2X_2Ru{=}CHR$ ($L = PCy_3$) and a terminal stryryl-ether olefin (Figure 2).[17] The issue was later enlarged by Grela et al. by dealing with the influence of the leaving group's rigidity on the catalyst's performance, which disclosed a remarkably

---

[10] Samojlowicz, C.; Bieniek, M.; Grela, K. Chem. Rev. 2009, 109, 3708-3742

[11] Scholl, M.; Ding, S.; Lee, C. W.; Grubbs, R. H. *Organic Letters* **1999**, 1, 6, 953-956

[12] Sanford, M. S.; Love, J. A.; Grubbs, R. H. *J. Am. Chem. Soc.* **2001**, 123, 6550

[13] Huang, J.; Stevens, E. D.; Nolan, S. P.; Peterson, J. L. *J. Am. Chem. Soc*. **1999**, 121, 2674

[14] Sanford, M. S.; Love, J. A.; Grubbs, R. H. *Organometallics* **2001**, 20, 531

[15] Claviere, H.; Petersen, J. L.; Nolan, S. P. *J. Org. Chem.* **2006**, 691, 5444-5447

[16] Ung, T., Hejl, A., Grubbs, R., H., Schrodi, Y., *Organometallics* **2004**, 23, 5399

[17] Kingsbury, J. S., Harrity, J. P. A.; Bonitatebus, P. J.; Hoveyda, A. H. *J. Am. Chem. Soc.* **1999**, 121, 791-799

coherence between the chelating carbene ligands and their stability/catalytic activity in olefin metathesis.[18]

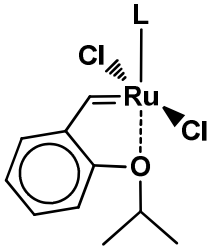

Figure 2. Hoveyda type initiator (**Hov-I**: L = PCy_3; **Hov-II**: L = NHC)

Further, additional insights were given by Grubbs-type metathesis catalysts bearing a *cis*-dichloro arrangement due to a chelating bis(di-*tert*-butylphosphanyl)methane (dtbpm) ligand.[19] These complexes feature - like all known and catalytically active Grubbs-type Ru carbene complexes - a square pyramidal ground-state geometry, where the ligands are arranged around the central transition metal. The halides and the neutral ligands occupy the square base, the carbene ligand the apical position.[39] The structural difference between *cis*- and *trans*-dichloro isomers lies in the position of the halides, which are placed side by side in *cis*-dichloro complexes and opposite to each other in the *trans*-dichloro counterparts (geometries are depicted in Figure 3, left).

The first ruthenium complexes with a *cis*-dichloro arrangement of the two halides were detected as side product in addition to the *trans*-isomer in 1993, when modifying the phosphine ligand of first well-defined $(PR_3)_2X_2Ru{=}CHR$ type complexes. Several works disclose their catalytic activity in metathesis, which is by far not as high as that of their *trans*-dichloro counterparts.[21] Further works have been aimed at synthesis[20] and thermodynamic behavior[6] of this kind of catalysts. However,

---

[18] Szadkowska, A.; Gestrein, X.; Burtscher, D.; Jarzembska, K.; Wozniak, K.; Slugovc, C.; Grela, K. *Organometallics* **2010**, 29, 117-124

[19] Hansen, S. M; Rominger, F.; Metz, M.; Hofmann, P. *Chem. Eur. J.* **1999**, 5, No. 2, 558

[20] Diesendruck, C. E.; Tzur, E; Ben-Asuly, A.; Goldberg, I.; Straub, B. F.; Lemcoff, N. G. *Inorg. Chem.* **2009**, 48, 10819-10825

the fundamental role of *cis*-dichloro complexes in the mechanism of ruthenium mediated olefin metathesis reactions is not yet well understood. In literature some examples for a *cis*/*trans* isomerization can be found, where, in solution, the more active *trans*-complex isomerizes to the thermodynamically favored *cis*-counterpart.[21] Other examples describe an activating isomerization in opposite direction, triggered by irradiation with UV light. [22] Theoretical, static density functional theory (DFT) studies of Poater et al. suggest a possible isomerization in both directions is possible, but associated with considerably high activation energies.[6]

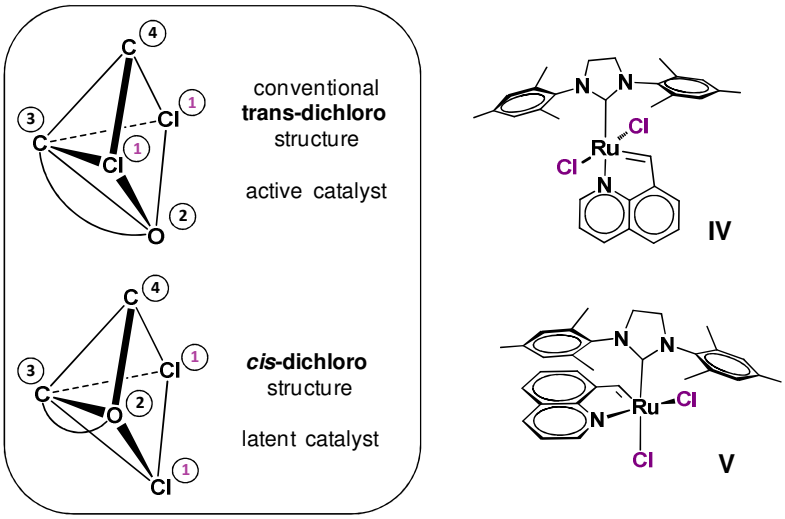

Figure 3. Coordination geometries of olefin metathesis catalysts (left), represented by ruthenium quinoline complexes **IV** (*trans*) and **V** (*cis)* (right)

Hence, the discovery of such *cis*-dichloro complexes led to a better understanding of the structure - activity relationship in Ru-catalyzed olefin metathesis,[4] what was i.a. elaborated in subsequent works of groups around Schrodi[19] and Grela.[21] These studies, concerning similar complexes, bearing a chelating aromatic N-heterocyclic ligand (like in Figure 3, right), showed a lower initiation rate for *cis*-dichloro complexes (like **IV**) than that of the *trans*-isomers (like **V**). Thus, it was demonstrated, that not only the chelate influences the catalyst's

[21] Barbasiewicz, M.; Szadkowska, A., Bujok, R.; Grela, K. *Organometallics* **2006**, 25, 3599-3604

[22] Asuly, A.; Aharoni, A.; Diesendruck, C. E.; Vidavsky, Y.; Goldberg, I.; Straub, B.; Lemcoff, N. G. *Organometallics* **2009**, 28, 4652-4655

performance but also the coordination geometry of the ligand environment (more detailed information can be found in chapter 2.2).

2.2. Mechanistic Impacts

For better understanding the olefin metathesis reaction, the basic mechanism and further, more detailed impacts will be explained in this chapter. The major breakthrough happened in 1971,[23] when Chauvin proposed a mechanism of transition metal olefin metathesis which was found to be most persistent with the experimental observations[24] and remains generally accepted until today. Figure 4 illustrates the Chauvin mechanism, where a metal-carbene complex undergoes a [2+2] cycloaddition with an olefin, forming a metallacyclobutane intermediate. This metallacyclobutane decomposes by [2+2] retrocycloaddition, generating either the original species or a new olefin and alkylidene.

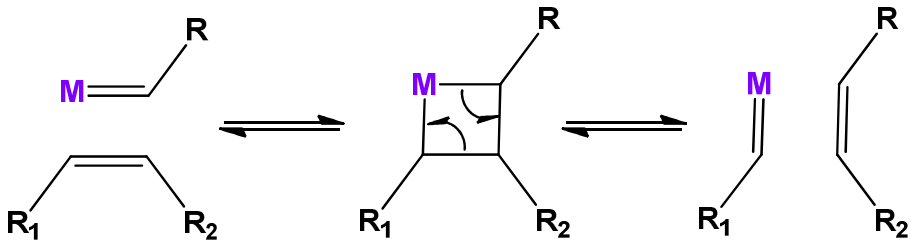

Figure 4. Mechanism of olefin metathesis

So far, all mechanistic scenarios of olefin metathesis were outlined for complexes bearing a *trans* dichloro arrangement like Grubbs-type complexes **I**, **II** and **III.** For the very first step, (the initiator entering in the catalytic circle) two limiting cases are proposed: an associative and a dissociative pathway.

The associative mechanism implies olefin coordination and an associated formation of an 18 electron complex, which subsequently rearrange to a *cis* arrangement of the coordinated olefin and the carbene ligand. In the dissociative route, a 14 electron species occurs after dissociation of the leaving group before olefin coordination can

[23] Hèrisson, J. L.; Chauvin, Y. *Makromol. Chem*. **1971**, 141, 161

[24] Grubbs, R. H.; Carr, D. D.; Hoppin, C.; Burk, P. L. *J. Am. Chem. Soc*. **1976**, 3478-3483

happen. Although reality may be somewhere between these two pathways, extensive kinetic studies on complexes like **I** and **II**, rather support the dissociative pathway (depicted in Figure 5),[25] including the naked 14 electron species, which is commonly considered to be the actual active species. Further findings, like the stable 14 electron complexes in works of Grubbs et al.,[26] point to the fact, that a dissociative pathway is most likely.

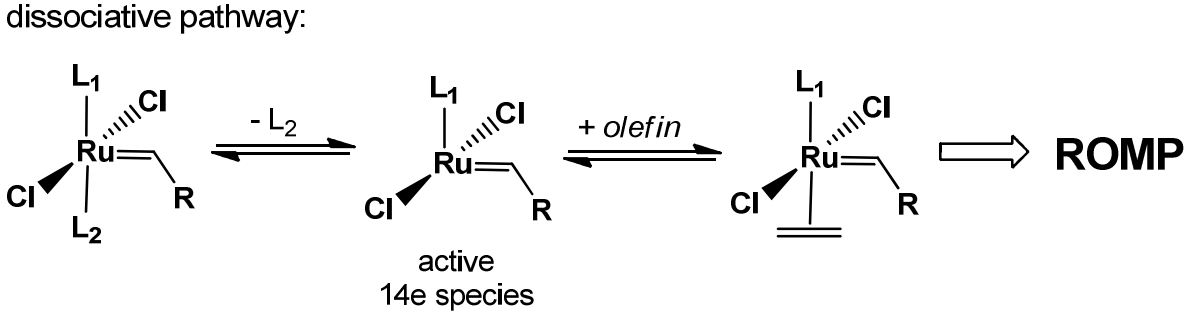

Figure 5. Dissociative pathway for olefin metathesis

Studies on Ru based complexes bearing bidentate quinoline ligands disclosed interesting mechanistic possibilities in connection with *cis and trans* dichloro isomers. It is proposed that, in case of a leaving group located *trans* to the strongly σ-donating NHC ligand (*trans*-dichloro complexes, Figure 3), the catalytically active 14-electron species (Figure 5) can be reached more quickly than in case of the *cis*-dichloro analogues.[27] Results of this work, however, debunk this thesis by predicting a *cis* to *trans* isomerization, by passing a cationic intermediate. After this rearrangement, the polymerization can start by running through the dissociative pathway and the Chauvin mechanism.

---

[25] Sanford, M. S.; Ulman, M.; Grubbs, G. H. *J. Am. Chem. Soc.* **2001**, 123 6543

[26] Sanford, M. S.; Henling, L. M.; Day, M. W.; Grubbs, R. H. *Angew. Chem. Int. Ed.* **2000**, 39, 3451

[27] Barbasiewicz, M.; Szadkowska, A., Bujok, R.; Grela, K. *Organometallics* **2006**, 25, 3602

3. Results and Discussion

Ruthenium based complexes bearing chelating ligands, such as 2-vinylbenzoic acid esters, feature a *cis*-dichloro structure. Internal ruthenium-oxygen chelation leads to a formation of a six-membered ring and forces the two chlorides into a *cis*-dichloro arrangement. In contrast to most of the commercially available catalysts, with a *trans* stereochemistry of the two halide ligands[39], this *cis*-dichloro compounds have not been examined that closely.

In this work initiators containing an electron donor functionalized benzylidene ester ligand were synthesized. The study should point out the role of the methoxy-functionalized chelating ligands and the influence of the different ester derivatives on the polymerization behavior. Furthermore, in the synthesis of *cis*-dichloro-(κ^2(C,O)-(2-iso-propyl ester-5-methoxy benzylidene)(1,3-bis(2,4,6-trimethylphenyl)-4,5-dihydroimidazol-2-ylidene) ruthenium a carbene containing side product was observed by ^{1}H NMR spectroscopy, that turned out to be a cationic complex. Derivatizations and further investigations on the cationic species brought new insights in the mechanistic behavior of *cis*-dichloro initiator. Presumably the cationic complex is an intermediate during the isomerization of *cis*-dichloro complex to the more active *trans*-counterpart, which will subsequently enter the olefin metathesis catalytic cycle. In this context, preparation procedures, ^{1}H, ^{13}C NMR and X-ray diffraction (XRD) characterizations of the novel ruthenium complexes and polynorbornenes prepared with them will be discussed.

3.1. Preparation of Initiators

3.1.1. Preparation of SPY-5-34 cis-Dichloro Complexes

M31 turned out to be an excellent staring material for the preparation of *SPY-5-34 cis*-dichloro ruthenium complexes bearing chelating carbenes. The fact, that the pyridine is not prone to re-coordinate with the 14 e^- intermediate

$(SIMes)(Cl)_2Ru(Ind)$,[28] leads, most probably, to a fast isomerization of the existing *SPY-5-31 trans*-dichloro structure towards the final isolated *SPY-5-34 cis*-dichloro structure.

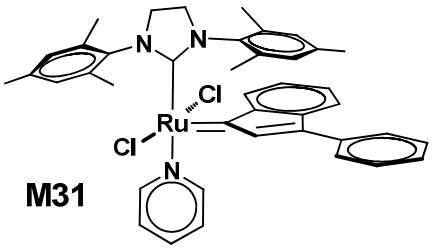

Figure 6. Starting material (**M31**) for synthesis of *cis* dichloro-ruthenium complexes bearing chelating ligands

SPY-5-34-cis-dichloro-(κ^2(C,O)-(2-ester-5-methoxybenzylidene)-(1,3-bis(2,4,6-trimethylphenyl)-4,5-dihydroimidazol-2-ylidene) ruthenium derivatives **1**-**3a** were prepared by a carbene exchange reaction with **M31** and a small excess of 2-vinyl-4-methoxy benzoic acid esters (**L6**-**L8**) according to literature (Figure 7).[39] The mixture was stirred at rt for one day, until full conversion was detected by TLC and the mixture turned from deep red to deep green. Generally, recrystallization with *n*-pentane was sufficient to gain pure products in satisfiable yields (35 - 98%).

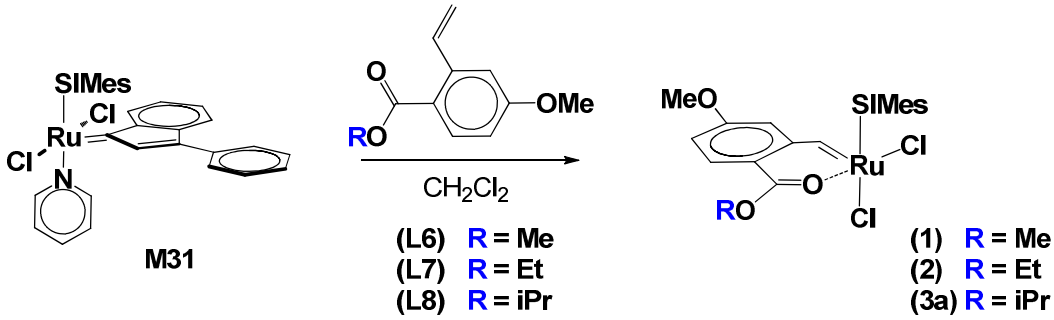

Figure 7. Typical ligand exchange reaction for preparing complex **1**-**3a**

[28] Claviere, H.; Petersen, J. L.; Nolan, S. P. *Journal of Organometallic Chemistry* **2006**, 691, 5444-5447

3.1.2. Preparation Cationic SPY-5-34 Ruthenium Complexes

In the procedure of **3a** a secondary product was found, which was separated by column chromatography on silica gel, using CH_2Cl_2/MeOH, 5:1 (v:v) with a yield of 5%. NMR spectroscopy and XRD proved the complex to be cationic, with a coordinated pyridine and a chloride as counter ion (**4**). Experiments to gain higher yields of complex **4** revealed that an excess of 3 eq. pyridine and extended reaction times (up to 5 days) are crucial to shift the equilibrium towards the cationic species (depicted in Figure 8). Thus, 37 % of the cationic species could be isolated.

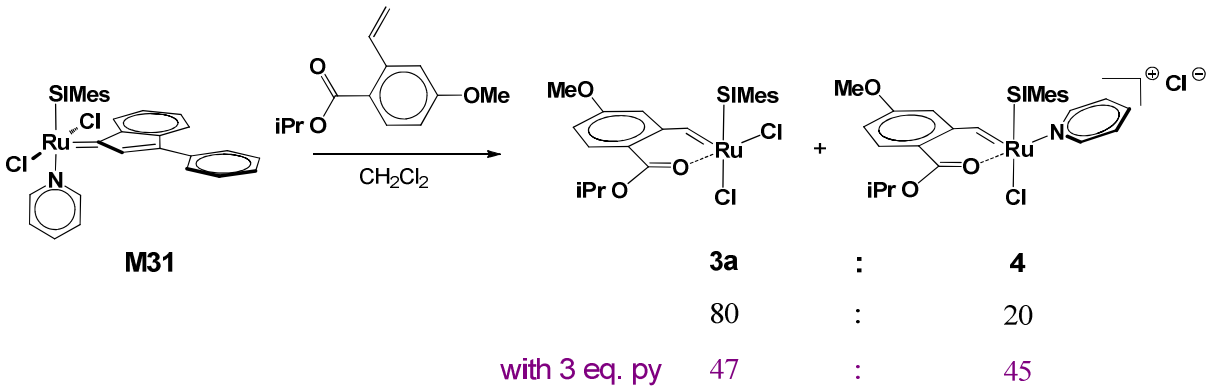

Figure 8. In the preparation of complex **3a** a secondary product was found, which turned out to be a cationic species with a coordinated pyridine (**4**). ^{1}H NMR evaluations of the crude product showed a shift of equilibrium towards the cationic product by adding an excess of pyridine

A second pathway, in which the cationic Cl^- ruthenium complex **4** was obtained, is presented in Figure 9. The addition of 50 eq. pyridine to complex **3a** in CH_2Cl_2 leads to 19 % of **4** after two hours (determined by NMR spectroscopy). Furthermore, it was observed, that complex **4** is not stable in solid state and even less in chlorinated solvent, such as CH_2Cl_2 or $CDCl_3$. The constant interaction of the counter anion (and - if present - the chlorines in solution) prompts a dissociation of the pyridine and a restoring of the starting compound **3a** to a certain percentage, which was not exactly determined. From these findings it can be deduced that complex **4** is not the favored state in thermodynamic equilibrium with **3a**.

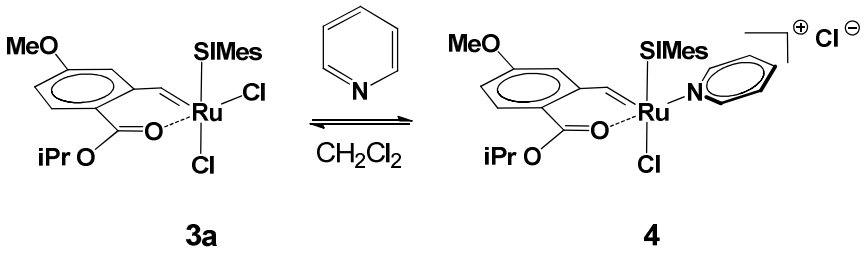

3a **4**

Figure 9. Second pathway to obtain complex **4**

To obtain more information about the influence of the counter ion on the catalyst's activity[29] of such complexes (like **4**), the chloride was substituted for the sterical bulkier PF_6 anion (see Figure 10). This would on the one hand prevent a re-coordination of the counter ion (for sterical reasons) and stabilize the cationic intermediate, which probably influences the formation of the metathesis-active 14 electron species.[30]

The exchange was accomplished in MeOH with complex **4** and a small excess of ammonium hexafluorophosphate. A bluish precipitate (yield: 65%) was formed, after stirring the reaction mixture for 30 min at room temperature.

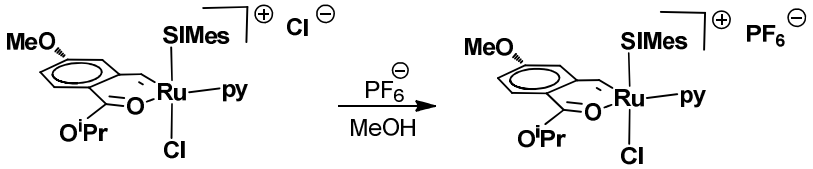

4 **5**

Figure 10. Procedure for counter ion exchange (**5**)

3.1.3. Preparation SPY-5-31 trans-Dichloro Ruthenium Complexes

For preparing the *SPY-5-31 trans*-dichloro Ru complex **3b**, the second generation complex **M2** (Figure 11) was used instead of the abovementioned **M31**.

---

[29] Volland, M. A. O.; Hansen, S. M.; Rominger, F.; Hofmann, P. *Organometallics* **2004**, 23, 800-816

[30] Sanford, M. S.; Ulman, M.; Grubbs, R. H. *J. Am. Chem. Soc.* **2001**, 123, 749-750

Compared to the fast dissociation of the labile pyridine in **M31** reactions, dissociation of the phosphine in **M2** is slow,[30] what - in this case - may retard a *trans* to *cis* isomerization.

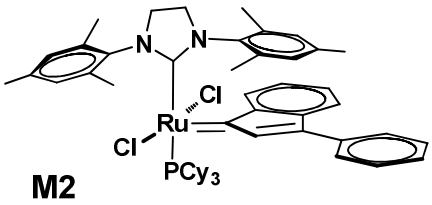

M2

Figure 11. Starting material for synthesis of *trans*-dichloro ruthenium complexes, bearing chelating ligands

As depicted in Figure 12, the *trans*-dichloro complex **3b** could be observed, when adding ligand **L8** to the second generation **M2**. In this case, the reaction mixture was stirred at room temperature for 18 h. Two products were separated by column chromatography, using CH_2Cl_2/MeOH, 20:1 (v:v). Unfortunately, some indenylidene and phosphine impurities could not be separated, but typical signals have identified the complex, which eluted first, as **3b** and the other complex as **3a**.

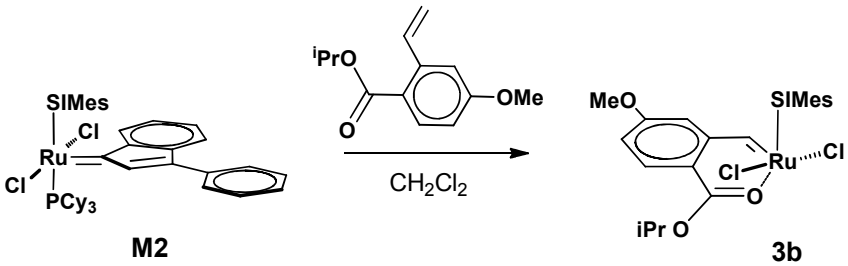

M2 **3b**

Figure 12. Procedure for preparing *trans*-dichloro complex **3b**

However, this method is avoided, because many disadvantages are implied, such as similar coordination tendencies of olefins and free phosphines. This might suppress the coordination of the olefin[31] and entail small yields. The addition of CuCl can inhibit the re-binding of the phosphine, by formation of a $CuCl{\cdot}PCy_3$ complex.

---

[31] Hoveyda, A.H.; Gillingham, D. G.; Van Velduizen, J. J.; Kataoka, O.; Barber, S. B.; Kingsbury, J. S.; Harrity, J. P. A. *Org. Biomol. Chem*. **2004**, 2, 8-23

Indeed, this complex leads to the next problem, because the copper-phosphine adduct may chelate the ruthenium center by bridging the chloride ligands,[32] which was actually observed in the ^{1}H-NMR spectrum of complex **3b** (see chapter 3.2.1).

3.2. Characterization of the Complexes

For characterization and identification of the novel Ru(II) complexes NMR spectra were recorded. X-ray structure determinations of selected compounds have been done.

3.2.1. NMR

Typically *cis*-dichloro complexes show a loss of symmetry, which can be explained by a slow rotation of the Ru(1)-C(1),[39] the N(1)-C(4) and the N(2)-C(13) bonds (Figure 13).[33]

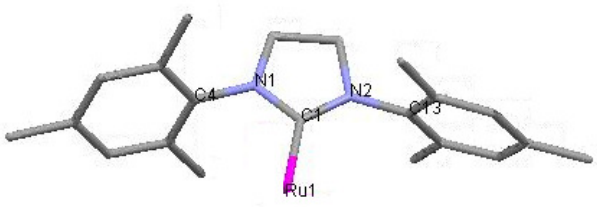

Figure 13. Labelling for some important SIMes-atoms

Thus, in ^{1}H NMR spectra of *SPY-5-34 cis*-dichloro Ru complexes a different signal pattern can be observed for the SIMes hydrogens, compared to *trans*-dichloro complexes. Figure 14 shows typical SIMes patterns in ^{1}H NMR spectra for *trans*- and *cis*-dichloro compounds, represented by **Hov-II** and **3a** respectively. Typical differences are represented by the mesityl signals (four *cis*-signals, one *trans*-signal),

---

[32] Dias, E. L., Nguyen, S. T.; Grubbs, R. H. *J. Am. Chem. Soc*. **1997**, 119, 3387-3897

[33] Burtscher Daniel, Thermally Switchable Initiators for Ring Opening Metathesis Polymerization, Diploma Thesis, Graz, 2004

the H_2Im signals (three *cis*-signals, one *trans*-signal) and the mesityl-C*H*$_3$ signals (six *cis*-signals, one *trans*-signal).

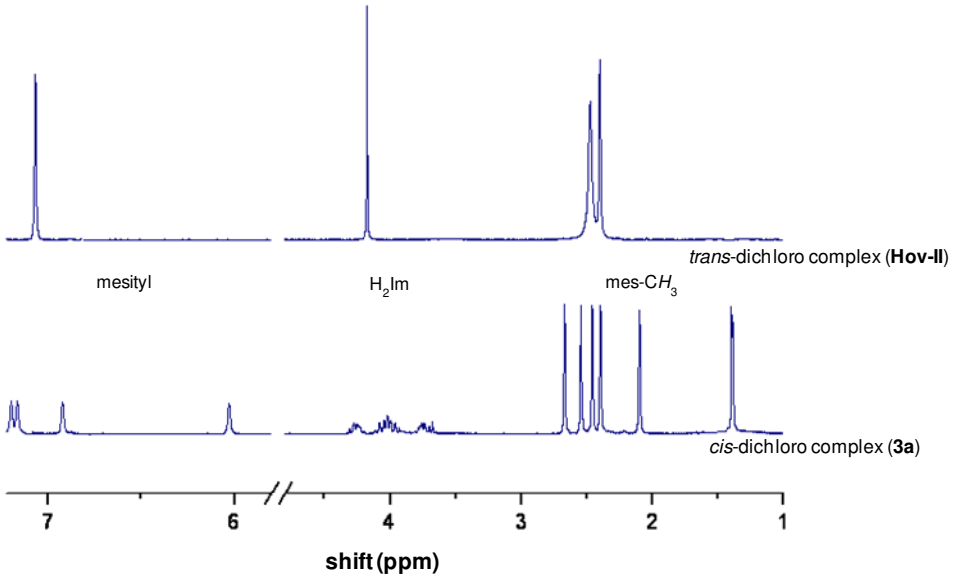

Figure 14. Different signal patterns for SIMes hydrogens in NMR spectra (300Hz, $CDCl_3$) of *trans*- (above) and *cis*- (below) dichloro ruthenium complexes. Solvent and other ligand peaks were removed for clarity

The ^{1}H-NMR spectrum of the isopropyl complex **3a**, depicted Figure 15, is also representative for the other *SPY-5-34* – dichloro – (κ^2(C,O)-(benzylidene-2-ester)-(1,3-bis(2,4,6-trimethylphenyl)-4,5-dihydroimidazol-2-ylidene)-ruthenium derivatives (**1**, **2**), because the influence of the ester residue onto the remaining hydrogens is negligible small (0.01 ppm). Further information can be gained from the spectrum below.

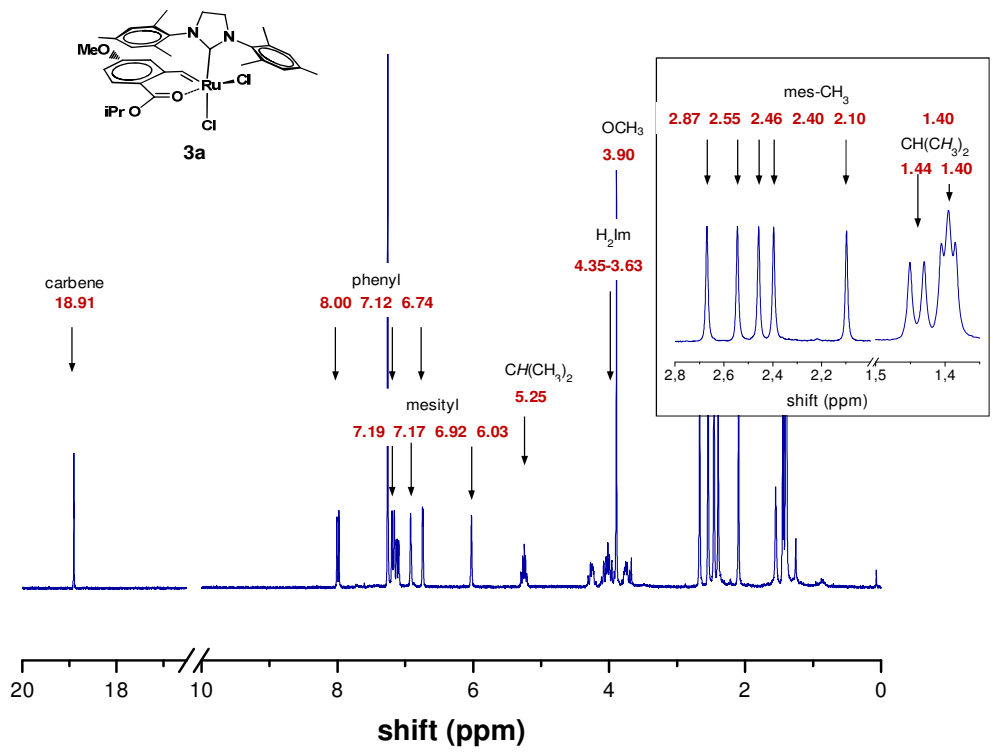

Figure 15. ^{1}H NMR spectrum (300 Hz, $CDCl_3$) of complex **3a**

In the preparation of **3a** a further carbene containing product was obtained (c.f. 3.1 and 4.3.1.3). This secondary product was isolated by column chromatography and identified by NMR spectroscopy. Conspicuities of this new compound, include three new signals, which correlate to one pyridine molecule, a highfield shift of the carbene resonance from 18.90 (**3a**) ppm to 17.92 ppm (prompted by the stronger linkage between Ru and py, compared to the analogue Ru(1)-Cl(1) bond, c.f. chapter 3.2.2), and a new signal pattern for the mesityl- (two signals), mesityl-CH_3 (three signals) and H_2Im- (one signal) hydrogens (see Figure 16). This set of signals is typical for a repeal of rotation hindrance for the Ru(1)-C(1) bond whereby the hindered rotations for the N(1,2)-C(4,13) bonds are maintained.

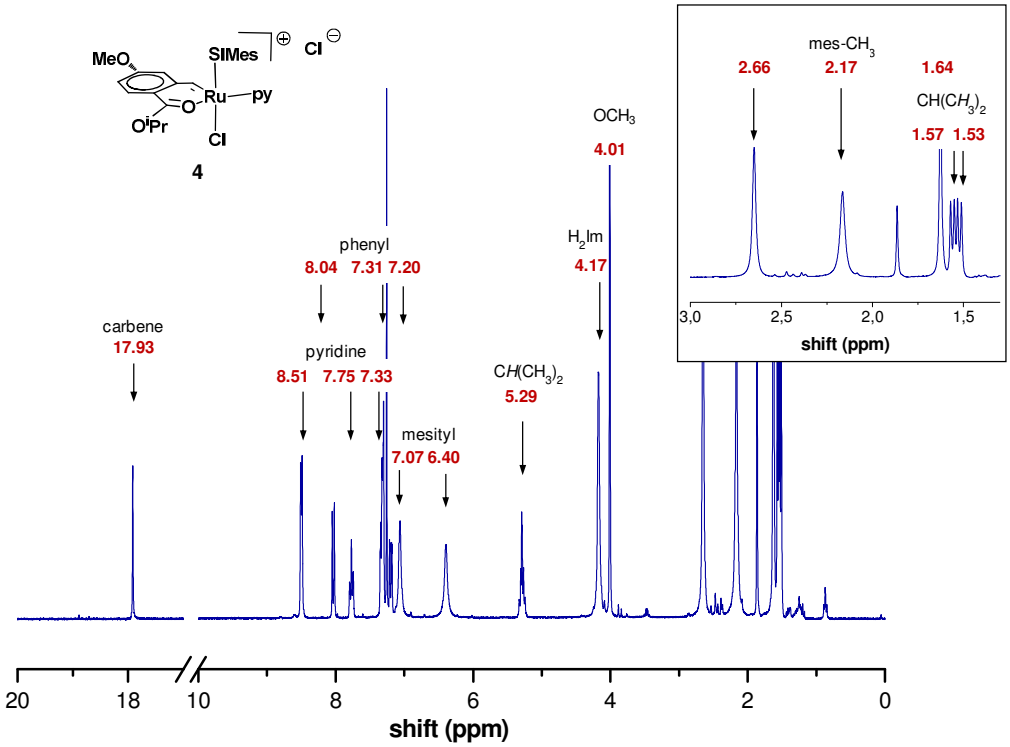

Figure 16. ^{1}H NMR spectrum (300 Hz, $CDCl_3$) of the cationic Cl^- ruthenium complex (**4**)

In further experiments the chloride counter ion was exchanged for the sterical bulkier PF_6 anion. The chloride was removed as unsolvable precipitate and removed by filtration (see chapter 4.3.3.2). One consequence of this substitution would be, that an interaction between the counter ion and the complex is inhibited - leading to differences in the polymerization behavior. Impacts of the PF_6 anion on the ^{1}H NMR signals are a highfield shift of the carbene hydrogen from 17.92 to 17.87 ppm and a new signal pattern of the SIMes ligand suggesting a hindered Ru(1)-C(1) rotation. This time, however, one N-C rotation is unhindered, resulting in a mes-C*H*$_3$ signal ratio of 1:2:1:1:1. Further, a noticeable broadening of these signals is visible, probably caused by an inequivalent rotation of the ligand, caused by the sterical bulky PF_6 ligand (see Figure 17).

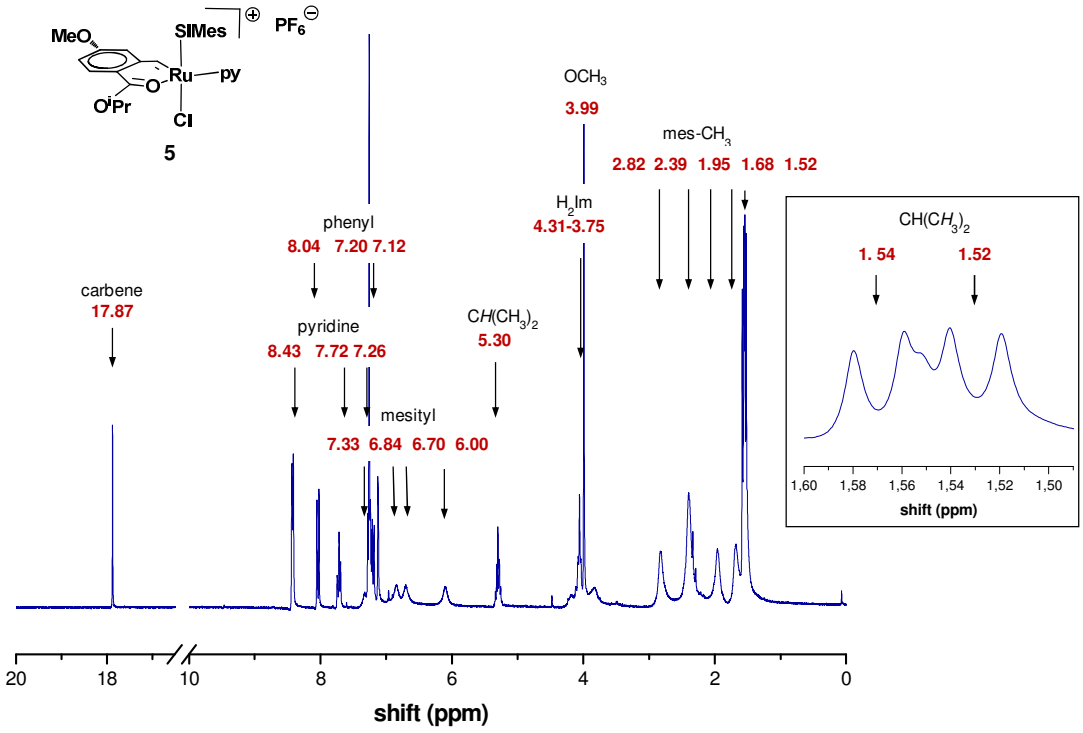

Figure 17. ^{1}H NMR spectrum (300 Hz, $CDCl_3$) of the cationic PF_6^- ruthenium complex **5**

In order to get evidence about the correlation between the *trans*-dichloro complex (**3b**) and the newfound, carbene containing product, that occurred in the ^{1}H NMR spectrum during polymerization with the cationic initiator **4** at 18.71 ppm the *trans*-initiator was isolated and characterized (detailed information in chapter 3.3.4). For preparing complex **4**, we started from second generation ruthenium complex **M2**, which suppresses a *trans* to *cis* isomerization (c.f. 3.1). In the ^{1}H-NMR spectrum (Figure 18), which was recorded 5 min after re-suspending the dried crystals in $CDCl_3$, the typical *trans* Cl-Ru-Cl signals were observed, with just one mesityl signal (7.10 ppm), one H_2Im signal (4.09 ppm) and the typical 2:1 ratio for the mes-CH_3 signals (2.49, 2.40 ppm). In addition to the clear signals assigned to the *SPY-5-31* *trans*-dichloro complex 3b, 3-phenyl-1H-inden-1-yliden (7.74-7.27, 6.95, 6.63 and 5.80 ppm) and tricyclohexylphosphine (1.99-1.55 ppm) were identified as side products.

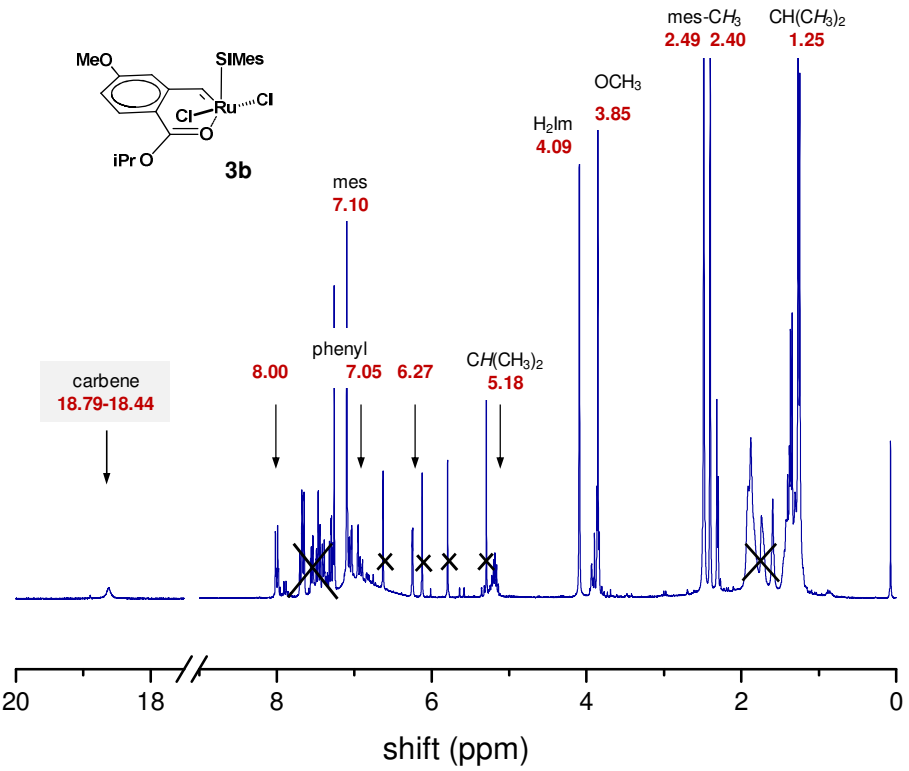

Figure 18. ^{1}H NMR spectrum (300Hz, $CDCl_3$) of the prepared *trans*-dichloro ruthenium complex (**3b**). Impurities were crossed out.

Unfortunately, the significant carbene signal emerged in the range of 18.79-18.44 ppm and not exactly at 18.71 ppm as in the ^{1}H NMR kinetic measurement with initiator **4** (c.f. chapter 3.3.4). Most probably the broad signal is the result of an interaction between the resulting, ill-defined CuCl phosphine complex and the *trans* Ru-complex **3b**.[32] This interaction leads to a broadening and a high field shift (up to 18.61-17.76 ppm after 21 h) of the carbene signal immediately. Another conspicuousness of the spectra (recorded 5 min, 1 h, 21 h after re-suspending the complex in $CDCl_3$) is, that the *trans* to *cis* ratio extends from 95:5 to 70:30 after 21 h an indication for the higher thermodynamic stability of the *cis*-complex **3a** (Figure 19).

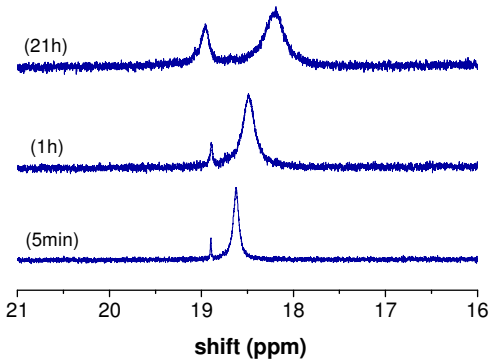

Figure 19. ^{1}H NMR spectra (300Hz, $CDCl_3$) of complexes **3a** and **3b**, recorded 5 min, 1 h and 21 h after resuspending the isolated *trans*-dichloro complex **3b** in $CDCl_3$

3.2.2. X-Ray-Structures

For stereochemical analysis, crystals were grown by Et_2O diffusion from a saturated solution of complex **1**-**3a** and **4** in CH_2Cl_2 and measured by single crystal X-ray diffraction. The structures of the ester derivatives are represented by the molecular geometry of **3a** (see Figure 20). As expected, the complexes bear the typical *cis*-dichloro geometry, which is close to a square pyramid (*SPY-5-34*). The base is formed by two chloro ligands, placed side by side (Cl(1), Cl(2)), the carbonyl oxygen (O(1)) and the carbon atom of the H_2Im ligand (C(1)). The carbene ligand (C(22)) occupies the apical position of the pyramid.

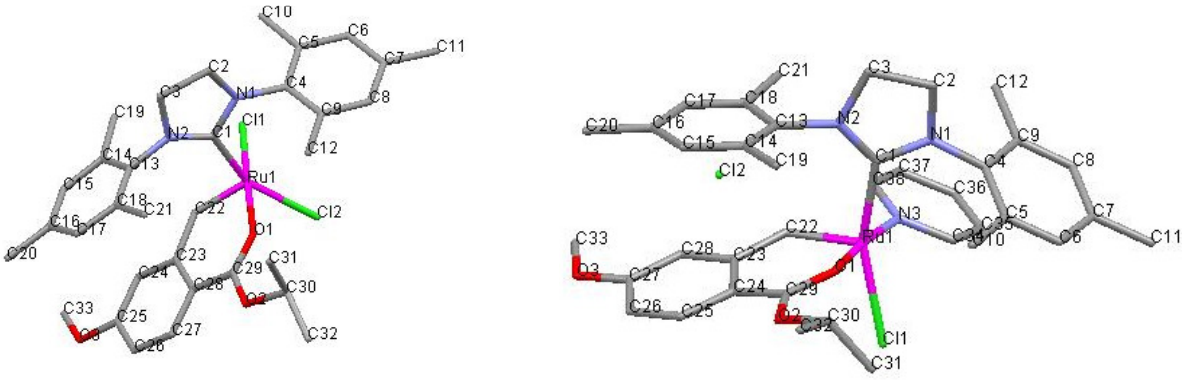

Figure 20. Molecular structure of **3a** (left) and **4** (right)

The abstraction of chlorine, forced by the addition of pyridine leads to replacement of the chlorine in the Cl(1) position by a pyridine molecule. Generally the structure remains the same for **3a** and **4**, as shown in Figure 20, Table 1 and Table 2.

Table 1. Selected bond lengths of **3a** and **4**

complex **3a**		complex **4**	
Ru-C(22)	1.8114(18) Å	Ru-C(22)	1.827(3) Å
Ru-C(1)	2.0201(18) Å	Ru-C(1)	2.034(3) Å
Ru-O(1)	2.0923(12) Å	Ru-O(1)	2.0739(18) Å
Ru-Cl(1)	2.3709(4) Å	Ru-N(3)	2.092(2) Å
Ru-Cl(2)	2.3643(5) Å	Ru-Cl(1)	2.3759(12) Å

Regarding the bond lengths of ruthenium with O(1), Cl(1) and Cl(2), it is consistent, that the chlorine with the higher bond length is abstracted and exchanged for a pyridine molecule. This substitution entails a stronger Ru-N(3) linkage (2.092(2) Å), compared to the Ru-Cl(1) bond length of complex **3a** (2.3709(4) Å). Further, this stronger Ru-N(3) bond elongates the benzylidene carbon bond length (Ru=CHR) of **4** (1.827(3) Å) slightly, compared to **3a** (1.8114(18) Å).

Table 2. Selected bond angles of **3a** and **4**

complex **3a**		complex **4**	
C(22)-Ru-C(1)	98.13(8)	C(22)-Ru-C(1)	98.03(11)
O(1)-Ru-Cl(2)	86.23(4)	O(1)-Ru-Cl(1)	85.63(6)
C(22)-Ru-O(1)	90.04(7)	C(22)-Ru-O(1)	90.57(10)
C(22)-Ru-Cl(2)	108.31(6)	C(22)-Ru-Cl(1)	104.82(8)
C(22)-Ru-Cl(1)	90.16(6)	C(22)-Ru-N(3)	94.98(11)
Cl(1)-Ru-Cl(2)	91.479(17)	N(3)-Ru-Cl(1)	90.68(7)

The bond angles of the neutral (**3a**) and the cationic Ru complex (**4**) resemble for the most part, as shown in Table 2. Two significant exceptions are the C(22)-Ru-Cl(1) and C(22)-Ru-N(3) angles, which differ from around four degrees, compared to their neutral analogues, probably due to sterical reasons.

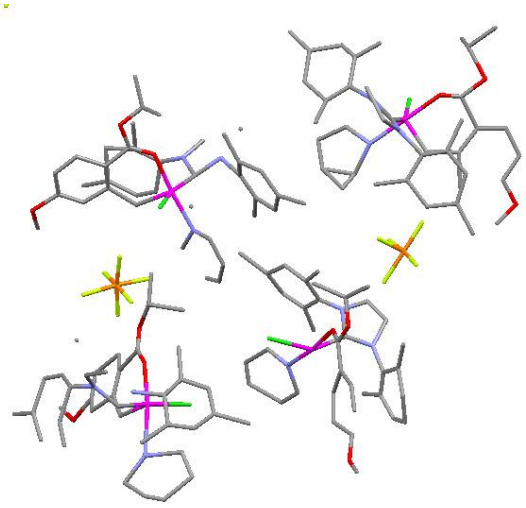

Figure 21. Molecular structure of **5**. The complex crystallizes in thin platelets and makes phase transformation at low temperatures

Attempts to get measurable crystals for XRD for complex **5** leaded to a tremendously effort, because the complex crystallizes (in saturated solution of **5** in CH_2Cl_2, layered with *n*-pentane) on the one hand in thin platelets, which grow on each other. Another problem arose, because the crystals are subjected to a phase transformation at low temperatures, what leads to a cleavage of the signal into several domains. These complications lead to an insufficient computation of the crystal structure. Nevertheless, the achieved structure confirms an anion exchange and the same constitution as described before for complex **4**.

3.3. ROMP Activity and Initiation Behavior

The catalytic activity of the prepared *cis*-dichloro complexes and their cationic derivatives were tested in ring opening metathesis polymerization (ROMP) with *endo*/*exo*-norbornendimethyl ester (**8**) as monomer (Figure 22).

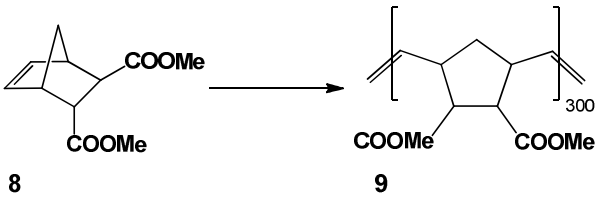

Figure 22. Polymerization procedure of monomer **8**

Standard conditions: M:I = 300:1, $c_{\mathcal{B}}$ = 0.1 mol/L, in CH_2Cl_2 at 40°C, in toluene at 80°C (procedure in chapter 4.4.1.1). The obtained polymers were analyzed by gel permeations chromatography (GPC) to determine the average molecular weight (number molecular weight, M_n), which will allow an indirect comparison of initiation rate to propagation rate constants (k_i/k_p) (1).

$$MWD \approx {kp}/{ki} \qquad (1)$$

Further, conversion was followed by NMR spectroscopy (M:I =70:1 for **1**-**3a** and **4**; M:I =5:1 for **3a**, **4** and **5**) to gain additional information about the catalytic activity.

3.3.1. ROMP Activity of cis-Dichloro Ruthenium Complexes

GPC analysis of polymers, catalyst by the *cis*-dichloro ester derivatives **1**-**3a** feature characteristic results for this kind of complexes.[4,39] For example, the conventional **M31** affords low molecular weight distribution (PDI ≤ 1.1) and effective molecular weights, close to the calculated molecular weight. This is the result of a high initiation and a high propagation rate constant. Figure 23 discloses the differences between **M31** and the latent *cis*-dichloro ruthenium complexes **1**, **2** and **3a**. These compounds lead to notably high M_n values, resulting from fast propagation, compared to the initiation (k_i/k_p is distinctly less than 1). Within the ester series the propagating species is equal for all initiators, so the determined M_n can be directly correlated to k_i. The influence of the ester on the initiation rate is small, but visible and increases from ethyl ester (**2**) < methyl ester (**1**) < *iso*-propyl ester (**3a**).

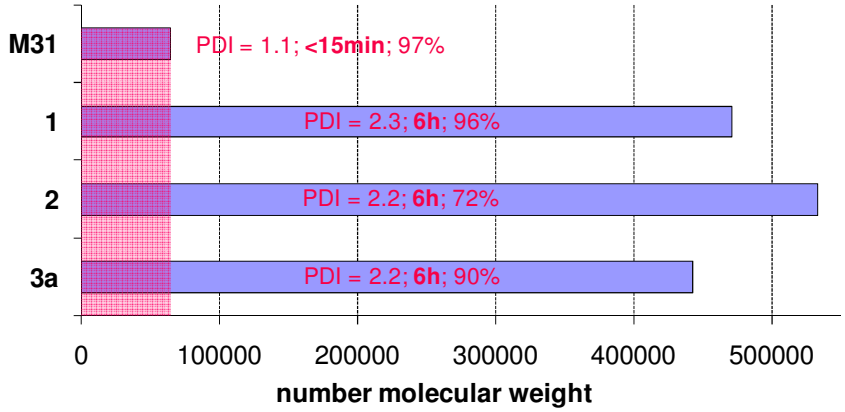

Figure 23. GPC results of polymer **9**, catalyzed with **M31**, **1**, **2** and **3a**

Figure 24 illustrates NMR kinetic measurements of initiators **1**-**3a**. The activities of the catalysts are represented by the half life ($t_{1/2}$), indicating 50% conversion from ethyl ester **2** ($t_{1/2}$ = 640 min) to methyl ester **1** ($t_{1/2}$ = 370 min) to *iso*-propyl ester **3a** ($t_{1/2}$ = 270 min). Compared to the abovementioned conclusion, results of both analyses comply with each other.

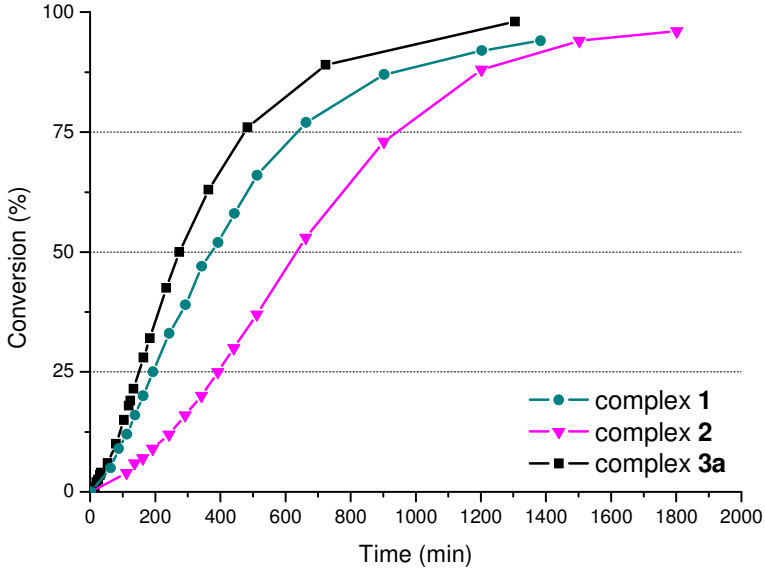

Figure 24. Monitoring polymerization of **8** with *SPY-5-31* trans dichloro ruthenium complexes **1**, **2** and **3a**

3.3.2. ROMP Activity of Cationic Ruthenium Complex 4

Results of polymerization with initiator **4** are not that easy to interpret if compared to results of the appropriate *cis*-dichloro complex **3a**. In this case, the propagating rate is not negligible any more, meaning that M_n is indirect proportional to the ratio of k_i/k_p. As depicted in Figure 25 the cationic effect of **4** leads to lower chain lengths, meaning k_i/k_p becomes higher, compared to **3a**. Approximated, that could eighter mean an decrease in the propagation or an increase in initiation rate. In order to distinguish between these two possiblities, polydispersity indices (PDI) and polymerization times have to be included. However, narrowing of the molecular weight distribution from 2.7 (**3a**) to 1.5 (**4**) and the decrease in reaction time from 4 h (**3a**) to 1 h (**4**) is more indicative for an increase of k_i.

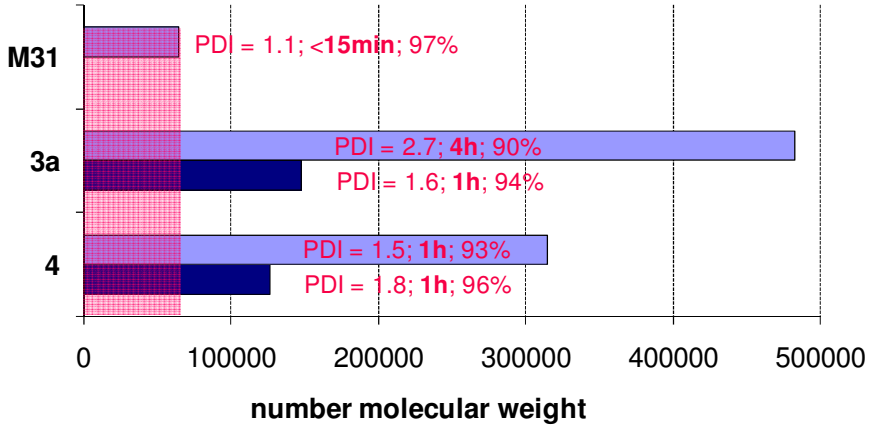

Figure 25. GPC characterization of polymer **9**, catalyzed by **M31**, **3a** and **4** under standard conditions (a) in CH_2Cl_2 at 40°C and (b) in toluene at 80°C

In addition to fast initiation times and low PDIs, ^{1}H NMR kinetic measurements with **3a** and **4** point out, that the cationic adduct **4** is more active with $t_{1/2}$ = 120 min, compared to $t_{1/2}$ = 270 min for compound **3a** (Figure 26). The diffrences in reactivity is striking and supposes a connection of the *SPY-5-34 cis*-dichloro compound and the cationic pyridine analogue **4**.

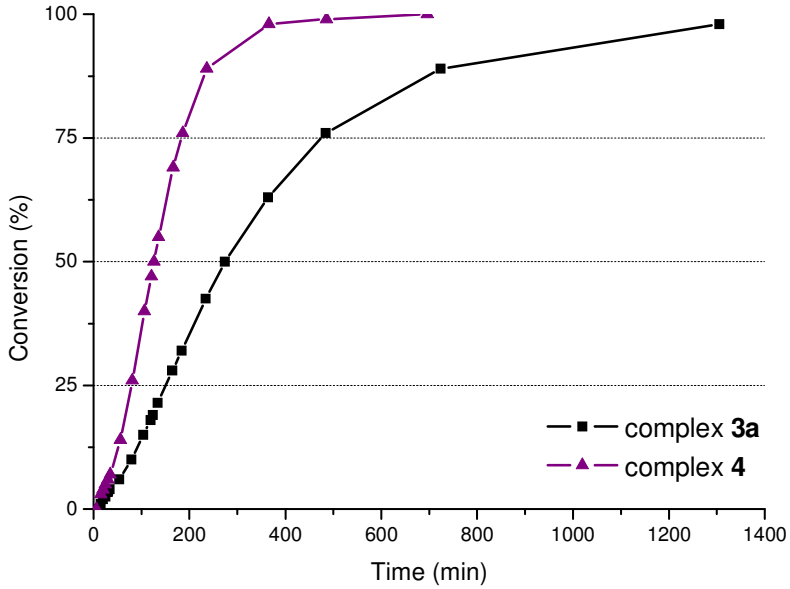

Figure 26. Polymerization of monomer **8** with complexes **3a** and **4** (M:I = 70:1), monitored by ^{1}H NMR (300 Hz, $CDCl_3$)

In literature[2,4,34,39] complexes with a *cis*-dichloro arrangement (like **3a**) are described to be very latent, compared to their *trans*-analogues, but mechanistic impacts are not yet disclosed. Considering the bond lengths of the *cis*-dichloro initiators (more details are found in 3.2.23.2.2), a halide abstraction is more likely than an aperture of the O→Ru chelate unfolding the initiator's non-chelated form. In this contribution, two plausible mechanistic pathways for an entrance into the catalytic cycle of olefin metathesis reactions are presented (Figure 27). Path A proposes a *cis* to *trans* isomerization, prompted by cationic intermediates like **4** (pyridine could be replaced by an electron donating solvent molecule), because pyridine (or the solvent molecule) would force the free chloride into the thermodynamically unfavored, but more active *trans* position. The second pathway (Path B) suggests a direct correlation between the cationic species and the catalytic activity. In this case pyridine liberation would lead to a resulting vacant coordination site (complex **10**) and hence to an entrance in the catalytic ROMP cycle. To differentiate between Path A and Path B, the chloride counter anion of complex **4** was exchanged for PF_6^-, what would block a re-coordination of the free chloride and consequently exclude Path A. In case of a

[34] Trnka, T. M.; Day, M. W.; Grubbs, R. H. Organometallics 2001, 20, 3845-3847

cationic active species (Path B), the exchange of the Cl^- would exclude an interaction between chloride and ruthenium and lead to a more active complex and therefore to accelerated polymerization.

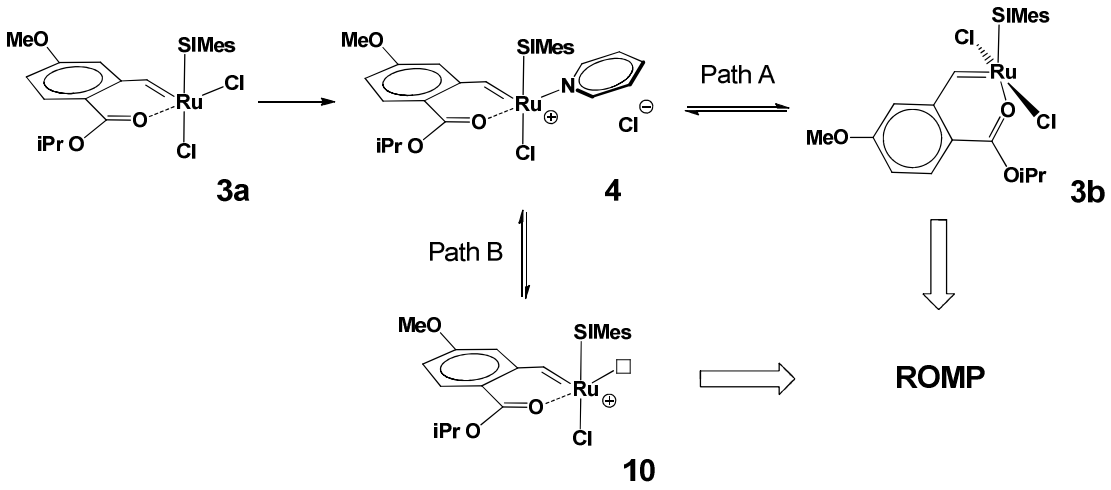

Figure 27. Possible mechanisms for the formation of the proposed ROMP active forms

3.3.3. ROMP Activity of Cationic Ruthenium Complex 5

Complex **5** was tested in ROMP under standard conditions in CH_2Cl_2 at 40 °C (M:I = 300:1, further information can be found in chapter 4.4.1.1). After 19 h reaction time a minimal conversion of 10 % was detected by ^1H NMR analysis Evaluation in the carbene region showed the typical carbene resonance at 17.87 ppm, meaning that the complex is very stable in chlorine containing solvents (Figure 28). The addition of chloride (benzyltriethylammonium chloride) results in a fully conversion of monomer **8** after 17 hours.

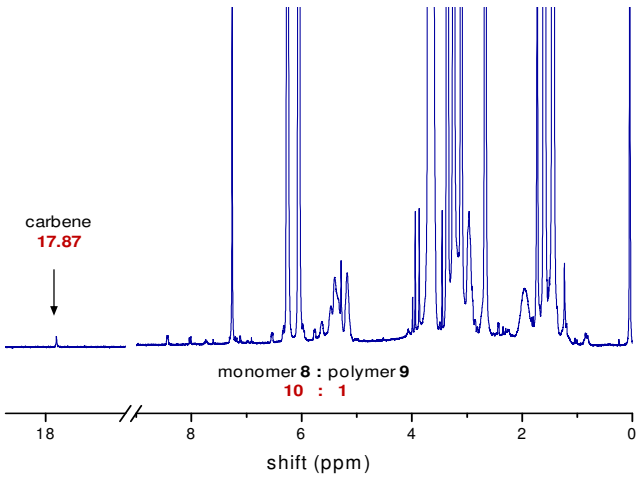

Figure 28. ^{1}H NMR spectrum (300 Hz, $CDCl_3$) of polymerization of monomer **8** with initiator **5** after 19 h (M:I = 300:1, c_8 = 0.1, CH_2Cl_2, 40°C)

The case under consideration confirmed an isomerization to the *trans* initiator **3b** and an associated entrance in the catalytic circle (Path A). The evidence for this is on the one hand the catalytic inertness (10 % conversion after 19 h) of complex **5**, which rules out the cationic intermediate **10** as the actual active species. Another proof for Path A concerns the addition of benzyltriethylammonium chloride, enabling a coordination of chloride in *trans* position to the second halide and a concomitant increase in reactivity (complete conversion after 17 h).

3.3.4. ^{1}H NMR Kinetic Measurement with 3a, 4 and 5

To confirm the validity of the abovementioned results, we finally conducted ^{1}H NMR kinetic measurements (300 Hz, $CDCl_3$) with initiator **3a**, **4** and **5** (M:I = 5:1) within the 20 ppm region. The propagation of the polymerization was monitored, by recording spectra every few hours at 21.5°C (procedure in chapter 4.4.1.3). Unfortunately, complex **4** has restored to complex **3a**. The actual ratio of cationic chloride complex **4** to *cis*-dichloro complex **3a** was 7:5. Anyway, the activity of the mixture with the cationic chloride complex **4** was significantly higher ($t_{1/2}$ = 17 h), than the activities of the *cis*-dichloro initiator **3a** ($t_{1/2}$ = 45 h) and the cationic PF_6 complex **5** (17 % conversion after 70 h). Subsequently, the addition of 3 equivalent benzyltriethylammonium chloride leads to completion of polymerization after further 26 h (Figure 29).

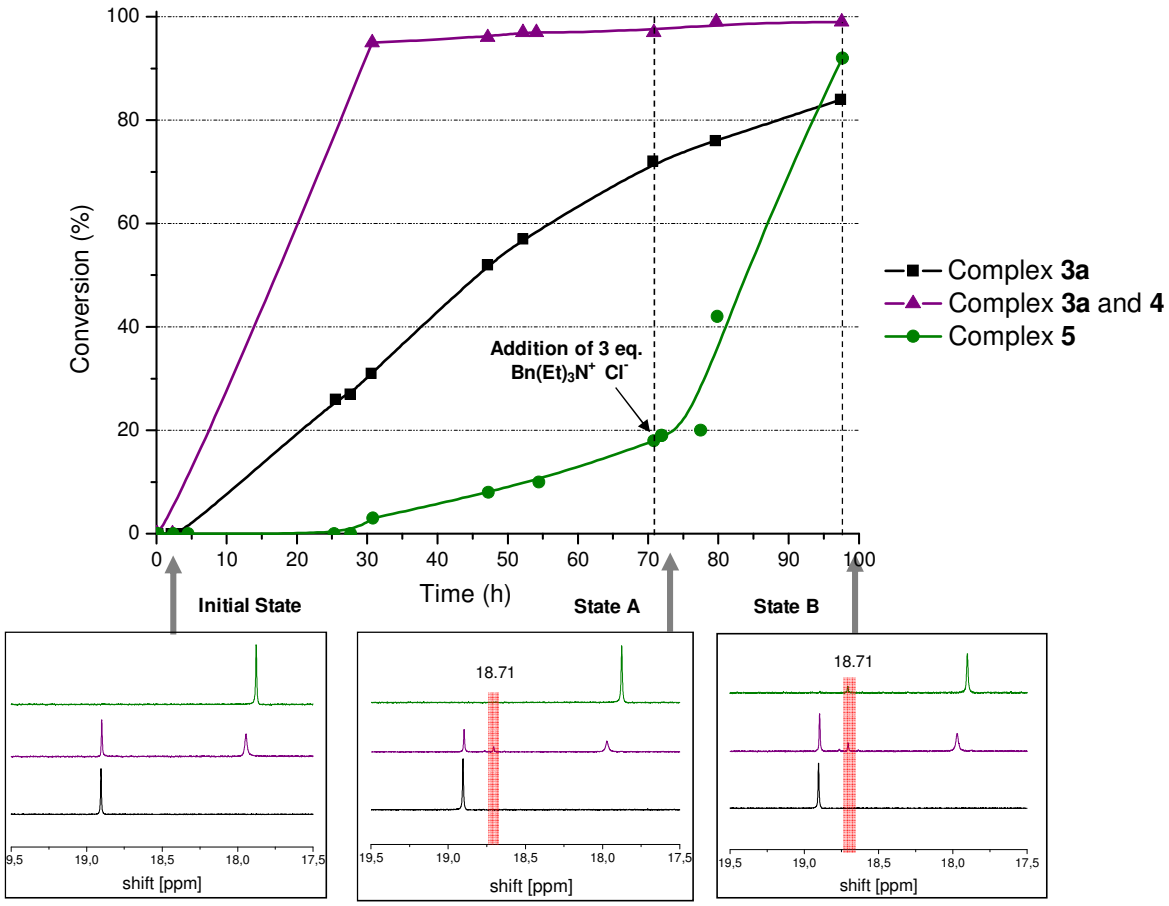

Figure 29. ^{1}H NMR kinetic measurement (300 Hz, $CDCl_3$) of polymerization of **8** with complexes **3a**, **4** and **5** (M:I = 5:1). New carbene signal at 18.71 ppm was assigned to active *trans*-dichloro complex **3b**

After having information about the catalytic activity, the attention was focused on the carbene region. Three states are outlined in Figure 29: the Initial state, State A (after 70 h) and State B (after 96 h). The initial carbene signals were found at 18.91 ppm for initiator **3a**, at 18.91 and 17.91 ppm for the mixture of **3a** and **4** and 17.87 ppm for complex **5**. In State A an additional peak appeared for **4** at 18.71 ppm, the other two compounds showed no conspicuities. After having added chloride salt to **5** (State B), the counter anion re-exchanged and the cationic Cl complex **4** was formed. This was detected by a downfield shift from 17.87 to 17.90 ppm and the appearance of two sharp mesityl signals at 7.09 and 6.41 ppm instead of four broad ones. In further consequence, a part of the free chloride re-coordinates to the ruthenium center, what was confirmed by the emergence of a singlet at 18.71 ppm (supposed to be complex **3b**) and traces of *cis*-dichloro ruthenium complex at 18.90 ppm. Another indication for the appearance of the *trans*-complex is visible, when comparing ^{1}H

NMR kinetic measurements with **4** and ^{1}H NMR spectrum of complex **3b**. Figure 30 shows that mainly the same signals occurred in both spectra, except for the carbene signal of initiator **3b**. It seems, that the ill-defined CuCl phosphine complex, which occur in the synthesis of the *SPY-5-31 trans*-dichloro ruthenium compound interacts with **3b** and leads to a broad signal from 18.79 to 18.44 ppm. (see chapter 3.2.1). Nevertheless, the complex was identified by the other significant peaks (e.g. ph^{6} at 6.27 ppm).

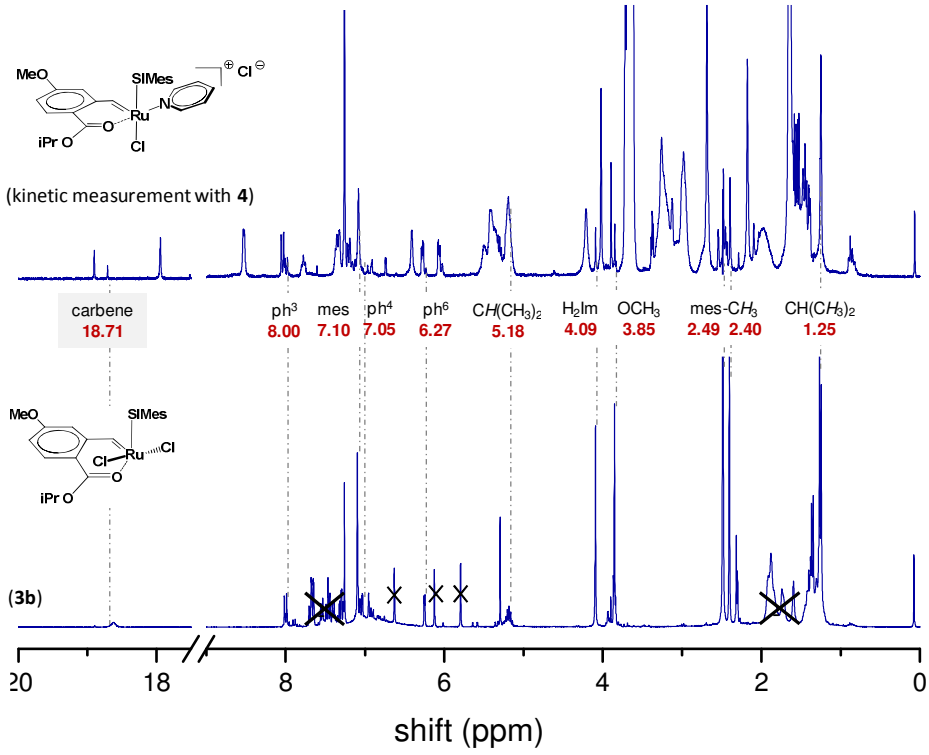

Figure 30. ^{1}H NMR spectra (300Hz, $CDCl_3$) of the prepared *trans*-dichloro ruthenium complex (**3b**, below) and *trans* complex, that arises during polymerization of monomer **8** from the cationic Cl complex (**4**, above). 3-Phenyl-1*H*-inden-1-yliden and tricyclohexylphosphine impurities were crossed out.

3.4. Insights in One-Pot synthesis of Cationic PF_6 Complex

3.4.1. Starting Material: cis-Dichloro Complex 3a

Another objective of this work was to find an alternative method to gain compound **5** from its neutral analogue **3a**. Therefore, complex **3a** and 50 eq. pyridine were

dissolved in dichloromethane and stirred for 2 days. Then $NaPF_6$ was added and the mixture reacted for five more days (procedure depicted in Figure 31).

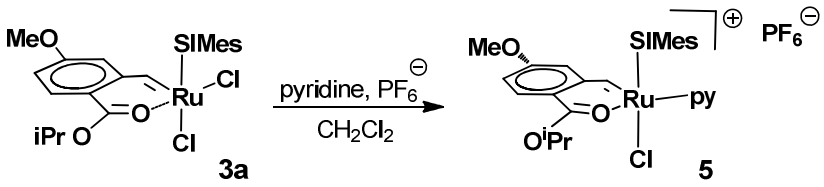

Figure 31. Alternative pathway to get complex **5**

The raw product was purified by column chromatography on silica gel, using CH_2Cl_2/MeOH, 20:1 - 5:1 (v:v). Three fractions were separated: (i) two carbenes were found, 80% at 19.38 ppm (red, not yet determined) and 20% at 17.88 ppm, what was identified as **5** (orange, see Figure 32), (ii) educt **3a**, with carbene at 18.91 ppm and (iii) cationic Cl complex **4**, with carbene at 17.92 ppm.

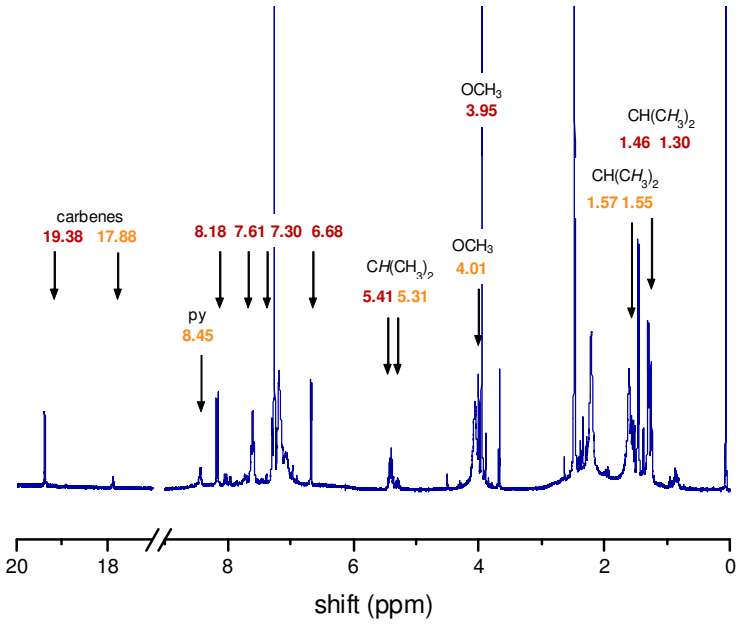

Figure 32. Cationic Complex **5** (orange), found in ^{1}H-NMR spectrum of first fraction (300Hz, $CDCl_3$)

3.4.1. Starting Material: cis-Dichloro Complex 6

In the synthesis of complex **6** also a cationic Cl side product was observed, however, in smaller yields. Hence, this compound was used for optimizing the one-pot synthesis with *SPY5-34 cis*-dichloro complex as starting material (see Figure 33). Generally the experiments were performed according the following procedure: 1 eq.

of complex **6**, 1 eq. PF_6^- salt (optional Ag^+ or Na^+) and optional 10 eq. pyridine were dissolved in solvent (CH_2Cl_2, CH_3NO_2 or CH_3CN) and stirred at room temperature for a certain time (more details are found in 4.3.3.4)

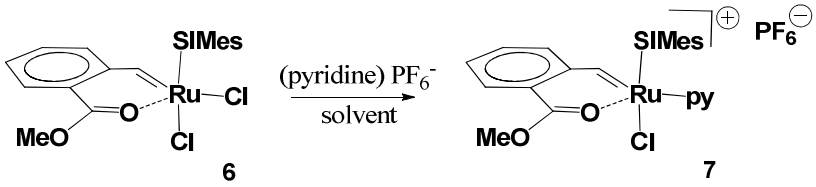

6 7

Figure 33. Alternative pathway for synthesis of the cationic PF_6 complex, starting from complex **6**

Two different test series were realized according to the abovementioned procedure to obtain product **7**: Series 1 with 10 eq. pyridine (detailed information can be found in Table 3 and Table 4) and Series 2 without pyridine (reaction conditions are summarized in Table 8 and Table 6).

Table 3. Reaction conditions of Series 1

	reaction conditions
Experiment 1	1.0 eq. 6, 1.2 eq. $NaPF_6$, 10 eq. py, CH_2Cl_2, 18 h, rt
Experiment 2	1.0 eq. 6, 1.2 eq. $AgPF_6$, 10 eq. py., CH_2Cl_2, 14 h, rt
Experiment 3	1.0 eq. 6, 1.2 eq. $NaPF_6$, 10 eq. py., CH_3NO_2, 18 h, rt

Table 4. Carbene signals of occurring products of Series 1, indicated by ^{1}H-NMR spectroscopy (300 Hz, $CDCl_3$)

	Experiment 1	**Experiment 2**	**Experiment 3**
before column	19.67 (57%) 19.49 (4%) 17.87 (39%)	19.68 (51%) 19.47 (7%) 17.87 (32%) further side products (10%): 18.84, 18.28, 17.61	19.48 (100%)
after column*	19.54 (94) 19.37 (6%) 17.85 (100%)	19.52 (93%) 19.37 (7%) 18.97 (11%) 18.73 (16%) 17.91 (48%) 17.57 (25%)	19.48 (100%)
after 6 days	19.32 (65%) 17.86 (35%) x	x	19.37 (78%) 17.86 (22%)

Generally, in the NMR spectra of experiments 1-3 the same three carbene containing products emerged, which are denoted as **P1**, **P2** and **P3**. Regretfully, the desired product **7** was not identified. The flow diagram of experiment 1, depicted in Figure 34, is representative for Series 1 and exposes the coherence between the three products **P1**-**P3**.

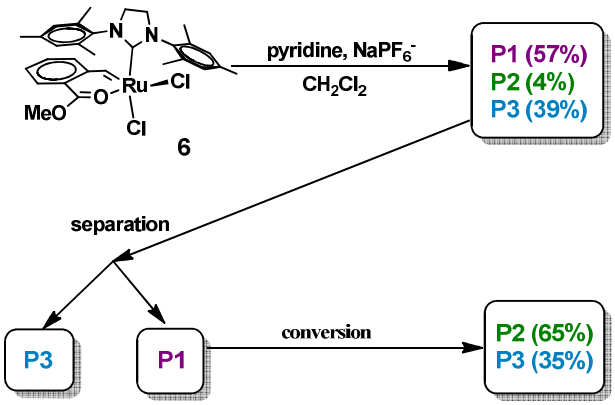

Figure 34. Flow diagram for experiment 1

Next it was tried to assign the ^{1}H NMR shifts and identify the novel complexes. Therefore, separation was carried out by column chromatography. In Fraction 2 a blue product (**P3**) was found, that showed narrow and well interpretable peaks. This complex turned out to be analogue to initiator **4**, with a similar carbene signal at 17.86 ppm, a coordinated pyridine and two mesityl signals at 6.98 and 6.41 ppm (Figure 35).

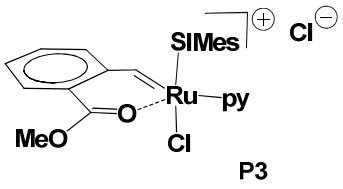

Figure 35. Structure of product **P3**

Interpretation of Fraction 1 (containing **P1**) is rather speculative: particular characteristics (see spectrum in Figure 36) involve a shift from 19.67 (raw product) to 19.54 ppm and a “greasing” in the pyridine region, that could be caused either by

equilibrium between free and coordinated pyridine or by a hindered, inequivalent rotation of the coordinated pyridine. Furthermore, the fact that **P1** distributes to **P2** (19.32 ppm) and **P3** (17.86 ppm) within six days, indicates an equilibrium between the unidentified complex **P2** and the cationic complex **P3**. To all appearances some - not yet allocated - interactions are causing a highfield shift in the carbene region from 19.64 (raw product) to 19.54 (after column chromatography) to 19.32 ppm, suggesting **P1** and **P2** are the same complexes.

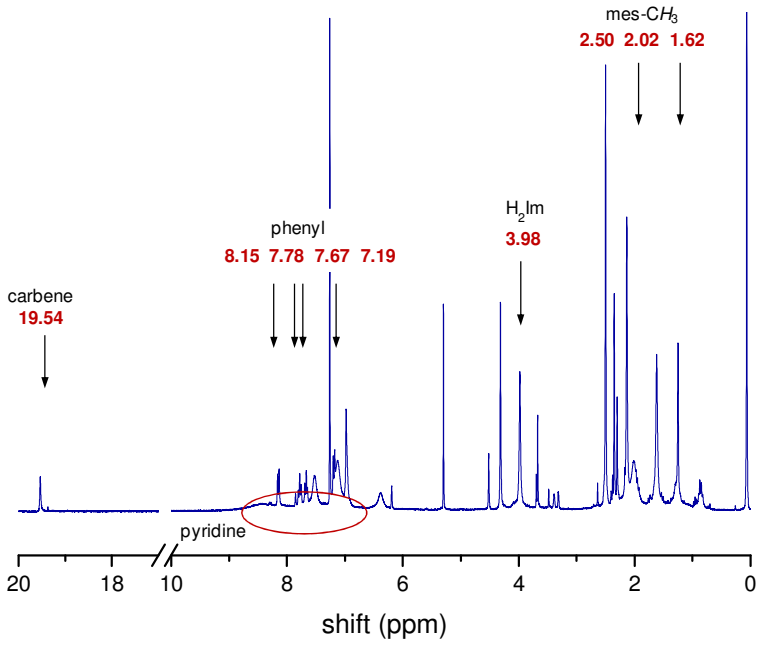

Figure 36. ^{1}H NMR spectrum (300 Hz, $CDCl_3$) of **P1**

Results of experiments 4-6 (Series 2) without the addition of pyridine exposed no reliability of this method, because neither the desired product nor a specific product could be isolated. Detailed information can be found in Table 5 and Table 6.

Table 5. Reaction conditions for Series 2

	reaction conditions
Experiment 4	1.0 eq. 6, 1.4 eq. $NaPF_6$, CH_3NO_2, 2 h, rt
Experiment 5	1.0 eq. 6, 1.1 eq. NaPF6, CH_3CN, 2 h, rt
Experiment 6	1.0 eq. 6, 1.0 eq. $AgPF_6$, CH_3CN, 16 h, rt

Table 6. Carbene signals of occurring products of Series 2, indicated by ^{1}H-NMR spectroscopy (300 Hz, $CDCl_3$)

	Experiment 4	**Experiment 5**	**Experiment 6**
before column	19.03 (bs, 38%) 17.85 (4%) 16.89 (11%) further side products (47%): 19.30, 18.79, 18.56, 18.47	19.06 (bs, 80%) 17.83 (7%) 16.96 (6%) further side products (7%): 18.45	18.97 (bs, 48%) 16.94 (36%) further side products (16%): 19.30, 18.56, 18.49, 17.58
after column	19.66 (49%)* 17.86 (26%) 17.39 (9%)	19.03 (51%) 17.81 (12%)	18.94 (57%) 16.93 (43%) 16.94 (100%)

4. Conclusion and Outlook

This work discloses in detail the mechanistic role of latent *SPY-5-34 cis*-dichloro complexes bearing a chelating ligand (various 4-methoxy-2-vinyl-benzoic acid ester derivatives) in ring opening metathesis polymerization (ROMP).

First, a negligible, sterical influence regarding the ester residue on the initiation rate constant in ROMP was found which increases in order of ethyl < methyl < *iso*-propyl. Far more striking was the fact that the presence of pyridine (and presumably other electron donating solvents) during the preparation of *SPY-5-34 cis*-dichloro complexes facilitates the dissociation of the labile chloride[35], *trans* to the electron donating O→Ru bond and leads to a cationic, pyridine containing complex with a chloride as counter anion. This newfound species was isolated, characterized and tested in ROMP under standard conditions. Compared to its *cis*-dichloro analogue, the novel complex featured a considerable increase in catalytic activity. Additionally, the compound was found to be an intermediate during the activating isomerization of the *SPY-5-34 cis*-dichloro precatalyst to its *SPY-5-31 trans*-dichloro counterpart. To validate the previous mentioned isomerization pathway, the Cl^- counter-ion was exchanged to the non coordinating hexafluorophosphate anion. Under tested reaction conditions the produced initiator turned out to be quite inactive, nevertheless switchable, by adding a chloride source. Herewith the indispensible role of the chloride counter-ion for the activity of the initiator is clearly demonstrated.

Summarizing, a novel concept for the latent *SPY-5-34 cis*-dichloro ruthenium complexes has been disclosed. Additionally, a switchable initiator system was found, which is worth being examined more closely.

---

[35] Tanaka, K.; Böhm, V. P. W.; Chadwick, D.; Roeper, M.; Braddock, D. C. *Organometallics* **2006**, 25, 5696-5698

Experimental Part

4.1. Instruments and Materials

All chemicals were purchased from commercial sources (Fluka, Sigma Aldrich or Alfa Aesar) and were used as received. **M2** ([1,3-Bis(2,4,6-trimethylphenyl)-2-imidazolidinylidene]dichloro-(3-phenyl-1H-inden-1- ylidene)(tricyclohexylphosphine) ruthenium(II)) and **M31** ([1,3-Bis(2,4,6-trimethylphenyl)-2-imidazolidinylidene] dichloro-(3-phenyl-1H-inden-1-ylidene)(pyridyl)ruthenium(II)) were procured from Umicore AG & Co. KG. Complex **6** and the accessory ligand were prepared analogously to literature.[39]

All preparation steps were performed under inert conditions (argon) with dry, degassed solvents, unless otherwise noted. For thin layer chromatography, TLC sheets from Merck (silica gel 60 on aluminium) were used.

Polydispersity indices (PDI) and molecular weight data were determined by gel permeation chromatography, using THF as eluent. The setting consists of the following arrangement: Merck Hitachi L6000 pump (delivery volume: 1 mL/min), separation columns of Polymer Standards Service (5µm grade size), refractive index detector form Wyatt Technology. For calibration polystyrene standards from Polymer Standard Service were used. NMR spectra (^{1}H, ^{13}C) were recorded on Bruker Avanze 300 MHz spectrometer and Varion INOVA 500 MHz (^{1}H NMR kinetic measurements), which were referenced to $SiMe_4$ and deuterated solvents (^{1}H, ^{13}C): $CDCl_3$ (7.26 ppm, ^{13}C to 77.0 ppm), CD_2Cl_2 (5.30 ppm, 53.52 ppm) and d^6 acetone (2.09 ppm, 205.87 ppm).[36] All deuterated solvents were obtained from Cambridge Isotope Laboratories Inc. X-Ray measurements were done on Burker Kappa APEX-2, using Mo Kα radiation.

---

[36] Gottlieb, H. E., Kotlyar, V., Nudelman, A., J. Org. Chem. **1997**, 62, 7512-7515

4.2. Preparation

4.2.1. Methoxy-2-vinyl benzoic acid iso-propyl ester

4.2.1.1. 2-Bromo-4-methoxy acetophenone

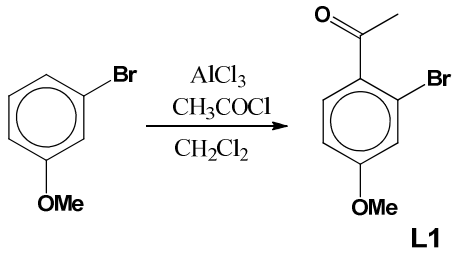

L1

Figure 37. Friedel Crafts acylierung (**L1**)

1-Bromo-3-methoxybenzene (5.0 g, 0.026 mol, 1.0 eq.) and aluminium chloride (4.378 g, 0.032 mol, 1.2 eq.) were dissolved in CH_2Cl_2 (50mL) and cooled to 0°C, then acetyl chloride was added dropwise. The reaction was stirred for 2 h at room temperature. Afterwards the reaction solution was poured on a mixture of ice water (50 mL) and HCl_{conc} (10 mL) and extracted with CH_2Cl_2 (2 x 100 mL). The organic layer was separated, washed with water (100 mL) and aqueous NaOH (10 w%, 100 mL). Further, the organic layer was dried with Na_2SO_4, filtered and evaporated. The oily residue was purified by column chromatography (pentane/Et_2O, 5:1, (v:v)by sampling the spot with R_f = 0.4). Yield: 3.64 g (59 %) clear oil.

Analytical data in accordance with published values.[37]
TLC: R_f = 0.4 (pentane/Et_2O, 5:1, (v:v)).

^{1}H-NMR (δ, 20°C, $CDCl_3$, 300 MHz): 7.59 (d, 1H, $^3J_{HH}$ = 8.7 Hz, ph^6), 7.15 (d, 1H, $^4J_{HH}$ = 2.5 Hz, ph^3), 6.88 (dd, 1H, $^3J_{HH}$ = 8.7 Hz, $^4J_{HH}$ = 2.5 Hz, ph^5), 3.84 (s, 3H, OCH_3), 2.62 (s, 3H, C=OCH_3).

---

[37] Takano, D.; Fukunaga, Y.;, Doe, M.; Yoshihara, K.; Kinoshita, T. *J. Heterocyclic Chem.* **1997**, 34, 1111-1114

4.2.1.2. 2-Bromo-4-methoxy benzoic acid

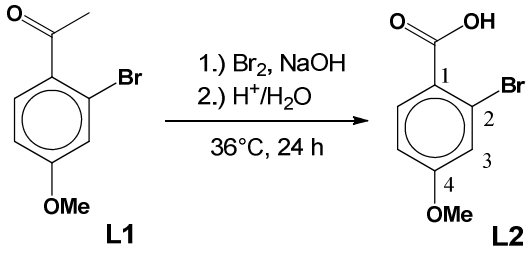

Figure 38. Haloform reaction (**L2**)

2-Bromo-4-methoxy-acetophenone (3.63 g, 15.8 mmol, 1.0 eq.) was added dropwise to a sodium hypobromit solution (bromine (2.93 mL, 56.9 mmol, 3.6 eq.) was dropped at 0°C in an aqueous NaOH-solution (20 w%, 50 mL)) and stirred at 36°C for 24 h. Na_2SO_3 (10 g in 40 mL) was added, then the reaction mixture was extracted with Et_2O. The aqueous phase was acidified with some drops of HCl_{conc}, the precipitate was filtered, washed with water and dried in vacuo. Yield: 2.60 g (71%) white solid.

Analytical data in accordance with published values.[38]
TLC: R_f = 0.4 (Cy/EtOAc, 3:1, (v:v)).

^{1}H-NMR (δ, 20°C, $CDCl_3$, 300 MHz): 8.04 (d, 1H, $^3J_{HH}$ = 8.8 Hz, ph^6), 7.23 (d, 1H, $^4J_{HH}$ = 2.5 Hz, ph^3), 6.90 (dd, 1H, $^3J_{HH}$ = 8.7 Hz, $^4J_{HH}$ = 2.5 Hz, ph^5), 3.87 (s, 3H, OCH_3).

---

[38] Wei, H.; Zhang, Y. J.; Wang, F.; Zhang, W. *Tetrahedron: Asymmetry* **2008**, 19, 482-488

4.2.2. 2-Bromo-4-methoxy benzoic acid esters

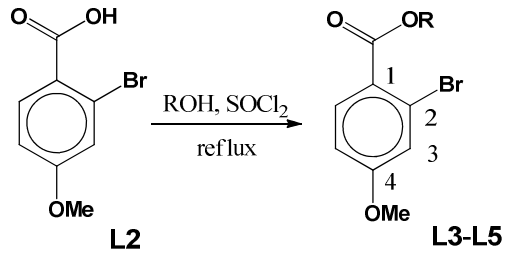

Figure 39. Esterification (**L3-L5)**

2-Bromo-4-methoxy benzoic acid (1.0 eq.) was suspended in the desired alcohol and cooled to 0°C, afterwards thionyl chloride (3.6 eq.) was added dropwise. The reaction mixture was stirred at reflux temperature until complete conversion was achieved. The excess of alcohol and thionyl chloride was distilled. The remaining liquid was dissolved in Et_2O (50 mL), water (50 mL), satured aqueous $NaHCO_3$ (50 mL) and extracted with Et_2O (2 x 100 mL). The organic layer was dried over Na_2SO_4, filtered, evaporated and dried in vacuo.

4.2.2.1.1. 2-Bromo-4-methoxybenoic acid methyl ester

The esterification of **L2** with methanol (**L3**) was done according to the general preparation in 4.2.2., using 2-bromo-4-methoxybenzoic acid (1.02 g, 4.41 mmol, 1.0 eq), thionylchlorid (1.89 g, 15.9 mmol, 3.6 eq.) and MeOH (8 mL) as the starting materials. Yield: 1.03 g (95%) clear oil.

Analytical data in accordance with published values.[38]

^{1}H-NMR (δ, 20°C, $CDCl_3$, 300 MHz): 7.85 (d, 1H, $^3J_{HH}$ = 8.8 Hz, ph^6), 7.18 (d, 1H, $^4J_{HH}$ = 2.5 Hz, ph^3), 6.85 (dd, 1H, $^3J_{HH}$ = 8.7 Hz, $^4J_{HH}$ = 2.5 Hz, ph^5), 3.89 (s, 3H, OCH_3), 3.82 (s, 3H, $COOCH_3$)

^{13}C-NMR (δ, 20°C, $CDCl_3$, 75 MHz): 165.83 (1C, C_q, *C*$OOCH_3$), 162.27 (1C, ph^4), 133.19 (1C, ph^{3,5,6}), 123.55, 123.32 (2C, C_q, ph^{1,2}), 119.8, 113.00 (2C, ph^{3,5,6}), 55.37 (1C, O*C*H_3), 52.11 (1C, COO*C*H_3).

4.2.2.1.2. 2-Bromo-4-methoxybenzoic acid ethyl ester

2-Bromo-4-methoxybenzoic acid ethyl ester (**L4**) was prepared analogously, using thionylchlorid (1.86 g, 15.7 mmol, 3.6 eq.), 2-bromo-4-methoxybenzoic acid (1.05 g, 4.35 mmol, 1.0 eq.) in EtOH (8 mL). Yield: 1.04 g (92%) yellowish oil.

^{1}H-NMR (δ, 20°C, $CDCl_3$, 300 MHz): 7.85 (d, 1H, $^{3}J_{HH}$ = 8.8 Hz, ph^{6}), 7.18 (d, 1H, $^{4}J_{HH}$ = 2.5 Hz, ph^{3}), 6.86 (dd, 1H, $^{3}J_{HH}$ = 8.7 Hz, $^{4}J_{HH}$ = 2.5 Hz, ph^{5}), 4.36 (q, 2H, $^{3}J_{HH}$ = 7.1 Hz, CH_2CH_3), 3.83 (s, 3H, OCH_3), 1.38 (t, 3H, CH_2CH_3, $^{3}J_{HH}$ = 7.1 Hz, CH_2CH_3)

^{13}C-NMR (δ, 20°C, $CDCl_3$, 75 MHz): 165.46 (1C, C_q, $COOCH_3$), 162.16 (1C, ph^{4}), 133.10 (1C, ph^{3,5,6}), 123.55, 123.32 (2C, C_q, ph^{1,2}), 119.69, 112.99 (2C, ph^{3,5,6}), 61.20 (1C, CH_2CH_3) 55.37 (1C, OCH_3), 52.11 (1C, $COOCH_3$), 14.23 (1C, CH_2CH_3)

4.2.2.1.3. 2-Bromo-4-methoxybenzoic acid iso propyl ester

The preparation of 2-bromo-4-methoxybenzoic acid *iso*-propyl ester (**L5**) was performed as mentioned above, using 2-bromo-4-methoxybenzoic acid (0.70 g, 3.03 mmol, 1.0 eq.) and thionylchlorid (1.3 g, 10.9 mmol, 3.6 eq) in *iso*-PrOH (8mL). Yield: 0.816 g (98%) yellowish oil.

TLC: R_f = 0.5 (Cy/EtOAc, 3:1 (v:v)).

^{1}H-NMR (δ, 20°C, $CDCl_3$, 300 MHz): 7.82 (d, 1H, $^{3}J_{HH}$ = 8.8 Hz, ph^{6}), 7.17 (d, 1H, $^{4}J_{HH}$ = 2.5 Hz, ph^{3}), 6.86 (dd, 1H, $^{3}J_{HH}$ = 8.7 Hz, $^{4}J_{HH}$ = 2.5 Hz, ph^{5}), 5.24 (m, 1H, $^{3}J_{HH}$ = 6.2 Hz, $CH(CH_3)_2$), 3.83 (s, 3H, OCH_3), 1.37 (6H, $^{3}J_{HH}$ = 6.2 Hz, $CH_2(CH_3)_2$).

^{13}C-NMR (δ, 20°C, CDCl3, 75 MHz): 165.10 (1C, C_q, $COOMe$), 162.05 (1C, C_q, ph^{4}), 132.99 (1C, ph^{6}), 124.29, 123.32 (2C, C_q, ph^{1,2}), 119.6, 113.01 (2C, ph^{3,5}), 68.90 (1C, C_q, $CH(CH_3)_2$), 55.67 (1C, OCH_3), 21.89 (2C, $CH(CH_3)_2$).

4.2.3. 4-Methoxy-2-vinyl benzoic acid esters

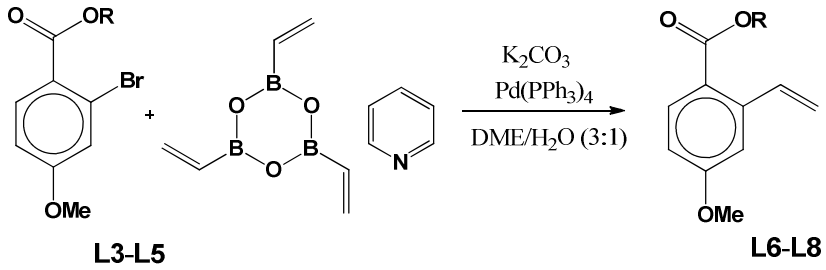

Figure 40. Suzuki coupling of 4-methoxy-2-vinyl benzoic acid esters (**L6-L8**)

2-Bromo-4-methoxy benzoic acid ester were prepared similar to literature[39] with (1 eq.), vinylboronic anhydride pyridine complex (1.2 eq.) and K_2CO_3 (2.0 eq) were dissolved in degassed DME/H_2O, 3:1 (v:v). $Pd(PPh_3)_4$ (0.104 g , 0.090 mmol, 0.03 eq.) was added and the reaction mixture was heated to 90°C and stirred for 1-2 d. The reaction mixture was quenched with water (10 mL). Et_2O (10 mL) was added and the organic layer was washed by shaking with aqueous HCl (10 w%, 3 x 100 mL) and aqueous, saturated $NaHCO_3$ (3 x 100 mL). The organic layer was dried with Na_2SO_4, filtered and evaporated and dried in vacuo.

4.2.3.1.1. 4-Methoxy-2-vinyl benzoic acid methyl ester

L6 was prepared according to the procedure above. 2-Bromo-4-methoxy benzoic acid methyl ester (1.03 g, 4.20 mmol, 1.0 eq.), vinylboronic anhydride pyridine complex (1.21 g, 5.04 mmol, 1.2 eq.) and K_2CO_3 (1.16 g, 8.40 mmol, 2 eq) were dissolved in 45 mL degassed toluene/EtOH/H_2O, 1:1:1 (v:v:v). $Pd(PPh_3)_4$ (0.146 g, 0.126 mmol, 0.03 eq.) was added and the reaction mixture stirred for 20 h at 90°C. Purification was done by column chromatography, using Cy/EtOAc, 6:1, (v:v). Yield: 0.561 g (85%) yellowish oil.

TLC: R_f = 0.5 (Cy/EtOAc, 3:1 (v:v))

---

[39] Slugovc, C.; Perner, B.; Stelzer, F.; Mereiter, K. *Organometallics* ***2004***, 23, 3622-3626

^{1}H-NMR (δ, 20°C, $CDCl_3$, 300 MHz): 7.91 (d, 1H, $^3J_{HH}$ = 8.7 Hz , ph^6), 7.58 (q, 1H, $^3J_{HH}$ = 11.1 Hz, C*H*CH_2), 7.04 (d, 1H, $^4J_{HH}$ = 2.6 Hz, ph^3), 6.83 (dd, 1H, $^3J_{HH}$ = 8.7 Hz, $^4J_{HH}$ = 2.6 Hz, , ph^5), 5.62 (dd, 1H, $^3J_{HH}$ = 17.4 Hz, $^4J_{HH}$ = 1.2 Hz, CHC*H*$_2$), 5.34 (dd, 1H, $^3J_{HH}$ = 11.0 Hz, $^4J_{HH}$ = 1.2 Hz, CHC*H*$_2$), 3.87 (s, 6H, OC*H*$_3$, $COOCH_3$)

^{13}C-NMR (δ, 20°C, $CDCl_3$, 75 MHz): 166.23 (1C, C_q, *C*$OOCH_3$), 162.47 (1C, C_q, ph^4), 142.37 (1C, ph^2), 136.39 (1C, *C*HCH_2), 132.71 (1C, ph^6), 120.77 (1C, C_q, ph^1), 116.37 (1C, *C*H_2CH), 112.75, 112.31 (2C, ph^{3,5}), 55.36 (1C, O*C*H_3), 51.77 (1C, $COOCH_3$)

4.2.3.1.2. 4-Methoxy-2-vinyl benzoic acid ethyl ester

Ligand **L7** was prepared as it was described in the procedure above, starting from 2-bromo-4-methoxy benzoic acid ethyl ester (1.04 g, 3.76 mmol, 1.0 eq.), vinylboronic anhydride pyridine complex (1.09 g, 4.51 mmol, 1.2 eq.) and K_2CO_3 (1.04 g, 7.52 mmol, 2 eq) were dissolved in degassed toluene/EtOH/H_2O, 1:1:1 (45 mL, v:v:v). $Pd(PPh_3)_4$ (0.130 g, 0.113 mmol, 0.03 eq.) was added and the mixture reacted for 2 d at 90°C. The raw material was purified by column chromatography, using Cy/EtOAc, 6:1 (v:v). Yield: 0.623 g (80%) yellowish oil.

TLC: R_f = 0.6 (Cy/EtOAc, 3:1 (v:v)).

^{1}H-NMR (δ, 20°C, $CDCl_3$, 300 MHz): 7.91 (d, 1H, $^3J_{HH}$ = 8.8 Hz , ph^6), 7.55 (q, 1H, $^3J_{HH}$ = 11.0 Hz, C*H*CH_2), 7.03 (d, 1H, $^4J_{HH}$ = 2.6 Hz, ph^3), 6.82 (dd, 1H, $^3J_{HH}$ = 8.7 Hz, $^4J_{HH}$ = 2.6 Hz, , ph^5), 5.61 (dd, 1H, $^3J_{HH}$ = 17.4 Hz, $^4J_{HH}$ = 1.1 Hz, CHC*H*$_2$), 5.34 (dd, 1H, $^3J_{HH}$ = 10.9 Hz, $^4J_{HH}$ = 1.2 Hz, CHC*H*$_2$), 4.33 (q, 2H, $^3J_{HH}$ = 7.2 Hz, C*H*$_2CH_3$), 3.86 (s, 6H, OC*H*$_3$, COO*C*H_3), 1.37 (t, 3H, $^3J_{HH}$ = 7.2 Hz, CH_2CH_3).

^{13}C-NMR (δ, 20°C, $CDCl_3$, 75 MHz): 166.78 (1C, C_q, *C*OOEt), 162.34 (1C, C_q, ph^4), 142.23 (1C, C_q, ph^2), 136.40 (1C, *C*HCH_2), 132.59 (1C, ph^6), 121.11 (1C, C_q, ph^1), 116.17 (1C, *C*H_2CH), 112.72, 112.33 (2C, ph^{3,5}), 60.59 (1C, *C*H_2CH_3) 55.31 (1C, O*C*H_3), 14.29 (1C, CH_2CH_3).

4.2.3.1.3. 4-Methoxy- 2-vinyl benzoic acid iso propyl ester

L8 was prepared analoguously to the abovementioned procedure. 2-Bromo-4-methoxy benzoic acid *iso* propyl ester (0.819 g, 3.00 mmol, 1.0 eq.), vinylboronic anhydride pyridine complex (0.867 g, 3.60 mmol, 1.2 eq.) and K_2CO_3 (0.828 g, 5.99 mmol, 2 eq) were dissolved in 20 mL degassed DME/H_2O, 3:1 (v:v). (R_f = xx in Cy/EtOAc, 3:1 (v:v)). Yield yellowish oil (0.561 g, 85%).

TLC: R_f = 0.x (Cy/EtOAc, 3:1 (v:v)).

^{1}H-NMR (δ, 20°C, $CDCl_3$, 300 MHz): 7.89 (d, 1H, $^3J_{HH}$ = 8.7 Hz , ph^6), 7.54 (q, 1H, $^3J_{HH}$ = 11.1 Hz, C*H*CH_2), 7.03 (d, 1H, $^4J_{HH}$ = 2.6 Hz, ph^3), 6.82 (dd, 1H, $^3J_{HH}$ = 8.8 Hz, $^4J_{HH}$ = 2.6 Hz, , ph^5), 5.61 (dd, 1H, $^3J_{HH}$ = 17.2 Hz, $^4J_{HH}$ = 1.2 Hz, CHC*H*$_2$), 5.34 (dd, 1H, $^3J_{HH}$ = 10.9 Hz, $^4J_{HH}$ = 1.2 Hz, CHC*H*$_2$), 5.21 (m, 1H, $^3J_{HH}$ = 6.2 Hz, C*H*$(CH_3)_2$), 3.87 (s, 3H, OC*H*$_3$), 1.35 (d, 6H, $^3J_{HH}$ = 6.2 Hz, CH(C*H*$_3)_2$).

^{13}C-NMR (δ, 20°C, $CDCl_3$, 75 MHz): 166.38 (1C, C_q, *C*OO^{i}Pr), 162.26 (1C, C_q, ph^4), 142.15 (1C, ph^2), 136.48 (1C, *CH*CH_2), 132.54 (1C, ph^6), 121.63 (1C, C_q, ph^1), 116.11 (1C, *C*H_2CH), 112.75, 112.31 (2C, ph^{3,5}), 68.06 (1C, *C*H$(CH_3)_2$), 55.37 (1C, O*C*H_3), 21.97 (2C, CH(*C*$H_3)_2$).

4.3. Ru(II)-Complexes

4.3.1. SPY-5-3 cis-Dichloro - Ruthenium Complexes

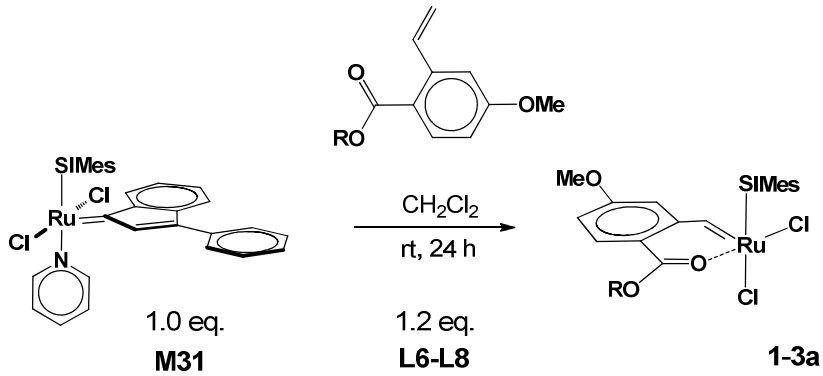

Figure 41. Typical procedure for the formation of *SPY-5-34 cis*-dichloro ruthenium complexes

In a Schlenk flask, **M31** (1.0 eq.) was dissolved in degassed, dry CH_2Cl_2. 1.2-1.5 eq. of the desired vinyl-benzoic acid ester derivative was added and the reaction mixture was stirred under argon atmosphere for 20 to 30 h, until the colour turned from deep red to deep green.[39] The solvent was removed in vacuo to 1 to 2 mL and precipitated with *n*-pentane. The dark green precipitate was filtered, washed with *n*-pentane and dried in vacuo.

4.3.1.1. (SPY-5-34) – Dichloro – (κ^2(C,O)-(2-methyl ester-5-methoxy benzylidene)-(1,3-bis(2,4,6-trimethylphenyl)-4,5-dihydroimidazol-2-ylidene)-ruthenium

Complex **1** was prepared analoguously to the procedure 4.3.1. **M31** (388 mg, 0.518 mmol, 1.0 eq) and 2-vinylbenzoic acid methyl ester (150 mg, 0.776 mmol, 1.5 eq.) in 10 mL CH_2Cl_2. Yield: 0.253 g (74%).green crystals.

TLC: R_f = 0.4 (CH_2Cl_2/MeOH, 10:1 (v:v)).

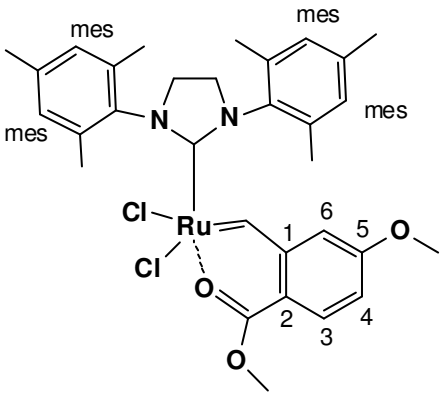

^{1}H-NMR (δ, 20°C, $CDCl_3$, 300 MHz): 18.92 (s, 1H, Ru=CH), 7.99 (d, 1H, $^3J_{HH}$ = 8.8 Hz, ph^3), 7.20, 7.17, 6.92, 6.02 (s, 4H, mes), 7.13 (dd, 1H, $^3J_{HH}$ = 8.9 Hz, $^4J_{HH}$ = 2.5 Hz, ph^4), 6.74 (d, 1H, $^4J_{HH}$ = 2.1 Hz, ph^6), 4.36 - 3.66 (m, 4H, H_2Im,), 4.03 (s, 3H, COOCH_3), 3.90 (s, 3H, OCH_3), 2.67, 2.53, 2.46, 2.40, 2.10, 1.37 (s, 18H, mes-CH_3).

^{1}H-NMR (δ, 20°C, CD_2Cl_2, 300 MHz): 18.85 (s, 1H, Ru=CH), 8.02 (d, 1H, $^3J_{HH}$ = 8.8 Hz, ph^3), 7.24-7.11, 6.91, 6.00 (s, 4H, mes), 7.16 (dd, 1H, $^3J_{HH}$ = 8.8 Hz, $^4J_{HH}$ = 2.7 Hz, ph^4), 6.77 (d, 1H, $^4J_{HH}$ = 2.5 Hz, ph^6), 4.31 - 3.64 (m, 4H, H_2Im,), 4.00 (s, 3H, COOCH_3), 3.90 (s, 3H, OCH_3), 2.60, 2.53, 2.41, 2.39, 2.06, 1.35 (s, 18H, mes-CH_3).

^{13}C-NMR (δ, 20°C, CD_2Cl_2, 125 MHz): 283.5 (1C, Ru=*C*H), 216.8 (1C, C_q, CNN), 176.5 (1C, C_q, COOCH), 166.3 (1C, C_q, ph^5), 144.6 (1C, C_q, ph^1), 139.9, 139.8, 138.56, 137.7, 137.1, 135.2 (6C, C_q, mes-C), 135.7 (1C, C_q, mes-N), 133.5 (1C, ph^3),

132.8 (1C, C_q, mes-N), 130.4, 129.5, 128.6 (4C, mes), 113.0 (1C, C_q, ph^2), 113.8, 112.14 (2C, ph^{4,6}), 55.9 (1C, O*C*H$_3$), 54.9 (1C, COO*C*Me), 51.02, 50.98 (2C, H_2Im), 21.1, 20.5, 19.8, 18.3, 17.9, 16.2 (6C, mes-*C*H$_3$).

4.3.1.2. (SPY-5-34) – Dichloro – (κ^2(C,O)-(2-ethyl ester-5-methoxy benzylidene)-(1,3-bis(2,4,6-trimethylphenyl)-4,5-dihydroimidazol-2-ylidene)-ruthenium

For preparing complex **2**, the same operation steps were used like described before. **M31** (347 mg, 0.601 mmol, 1.0 eq) and 2-vinylbenzoic acid ethyl ester (155 mg, 0.901 mmol, 1.5 eq.) were dissolved in 10 mL CH_2Cl_2 (R_f = 0.3 with CH_2Cl_2/MeOH, 10:1 (v:v)). Yield: 0.288 g (98%) green crystals.

TLC: R_f = 0.3 (CH_2Cl_2/MeOH, 10:1 (v:v))

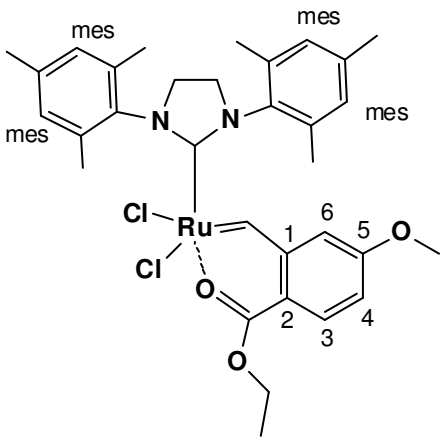

^{1}H-NMR (δ, 20°C, $CDCl_3$, 300 MHz): 18.92 (s, 1H, Ru=CH), 8.01 (d, 1H, $^3J_{HH}$ = 8.9 Hz, ph^3), 7.19, 7.17, 6.93, 6.03 (s, 4H, mes), 7.12 (dd, 1H, $^3J_{HH}$ = 8.8 Hz, $^4J_{HH}$ = 2.5 Hz, ph^4), 6.74 (d, 1H, $^4J_{HH}$ = 2.5 Hz, ph^6), 4.64 - 4.51 (m, 1H, C*H*$_2$CH$_3$), 4.41 - 4.30 (m, 1H, C*H*$_2$CH$_3$), 4.34 - 3.67 (m, 4H, H_2Im,), 3.90 (s, 3H, OC*H*$_3$), 2.68, 2.52, 2.46, 2.40, 2.10, 1.38 (s, 18H, mes-C*H*$_3$), 1.45, 1.43 (t, 3H, $^3J_{HH}$ = 6.7 Hz, CH$_2$C*H*$_3$)

^{13}C-NMR (δ, 20°C, CD_2Cl_2, 125 MHz): 283.5 (1C, Ru=*C*H), 217.6 (1C, C_q, CNN), 176.1 (1C, C_q, COOEt), 165.9 (1C, C_q, ph^5), 144.7 (1C, C_q, ph^1), 140.1, 139.6, 138.4, 138.0, 136.5, 135.1 (6C, C_q, mes-C), 135.6 (1C, C_q, mes-N), 133.3 (1C, ph^3), 132.3 (1C, C_q, mes-N), 131.0, 129.6, 129.5, 128.4 (4C, mes), 113.5 (1C, C_q, ph^2), 113.8, 111.9 (2C, ph^{4,6}), 64.2 (1C, *C*H$_2$CH$_3$), 55.7 (1C, O*C*H$_3$), 51.02, 50.98 (2C, H_2Im), 34.1 (1C, CH$_2$C*H*$_3$), 21.4, 20.7, 20.1, 18.3, 18.25, 16.3 (6C, mes-*C*H$_3$).

4.3.1.3. (SPY-5-34) - Dichloro - (κ^2(C,O)-(2-iso-propyl ester-5-methoxy benzylidene)-(1,3-bis(2,4,6- trimethylphenyl)4,5-dihydroimidazol-2-ylidene)-ruthenium

Complex **3a** was prepared according to the procedure in yy, using **M31** (165 mg, 0.221 mmol, 1.0 eq.) and 4-methoxy-2-vinyl-benzoic acid-i*so*-propylester (56.2 mg, 0.255 mmol, 1.2 eq.) in 5 mL CH_2Cl_2. Purification was set by column chromatography, using CH_2Cl_2/MeOH, 20:1 - 5:1, (v:v). Two fractions were separated, by sampling the spots with R_f = 0.3 (main product) and R_f = 0.1 (CH_2Cl_2/MeOH, 10:1, (v:v)). Yield: 60.2 mg (34%) dark green crystals and 8.9 mg (5%) turquoise crystals (side product).

TLC: R_f = 0.3 (CH_2Cl_2/MeOH, 10:1 (v:v)).

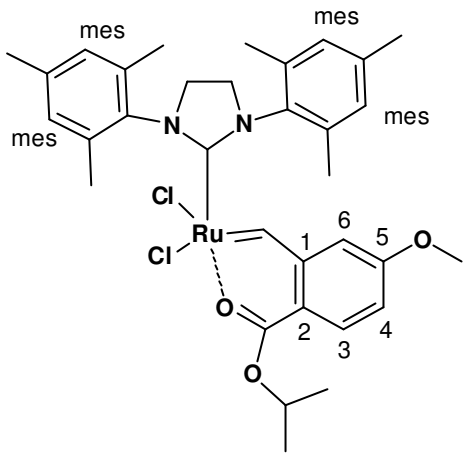

^{1}H-NMR (δ, 20°C, $CDCl_3$, 300 MHz): 18.91 (s, 1H, Ru=CH), 8.00 (d, 1H, $^3J_{HH}$ = 8.9 Hz, ph^3), 7.19, 7.17, 6.92, 6.03 (s, 4H, mes), 7.12 (dd, 1H, $^3J_{HH}$ = 8.8 Hz, $^4J_{HH}$ = 2.5 Hz, ph^4), 6.74 (s, 1H, $^4J_{HH}$ = 2.5 Hz, ph^6), 5.25 (m, 1H, C*H*$(CH_3)_2$, $^3J_{HH}$ = 6.2 Hz) 4.35-3.63 (m, 4H, H_2Im,), 3.90 (s, 3H, OC*H*$_3$), 2.87, 2.55, 2.46, 2.40, 2.10, 1.37 (s, 18H, mes-C*H*$_3$), 1.44, 1.40 (d, 6H, $^3J_{HH}$ = 6.0 Hz)

^{13}C-NMR (δ, 20°C, CD_2Cl_2, 75 MHz): Ru=CH (not observed), 217.7 (1C, C_q, CNN), 175.4 (1C, C_q, $COOCH_3$), 165.7 (1C, C_q, ph^5), 144.7 (1C, C_q, ph^1), 140.0, 139.6, 138.4, 136.3, 135.6, 135.1 (6C, C_q, mes-C), 135.6 (1C, C_q, mes-N), 133.2 (1C, ph^3), 132.4 (1C, C_q, mes-N), 131.0, 129.6, 129.5, 128.4 (1C, mes), 113.9 (1C, C_q, ph^2), 113.8, 111.9 (2C, ph^{4,6}), 72.1 (1C, *C*$H_2(CH_3)_2$), 55.7 (1C, O*C*H_3), 51.1, 51.0 (2C, H_2Im), 22.0, 21.8 (2C, CH(*C*$H_3)_2$), 20.7, 20.1, 18.3, 18.2, 16.4, 14.1 (6C, mes-CH_3).

4.3.2. SPY-5-31 trans-Dichloro - Ruthenium Complexes

4.3.2.1. Preparation of (SPY-5-31)-dichloro-(κ^2(C,O)-(2-iso-propyl ester-5-methoxy benzylidene)-(1,3-bis(2,4,6- trimethylphenyl)-4,5-dihydroimidazol-2-ylidene)-ruthenium

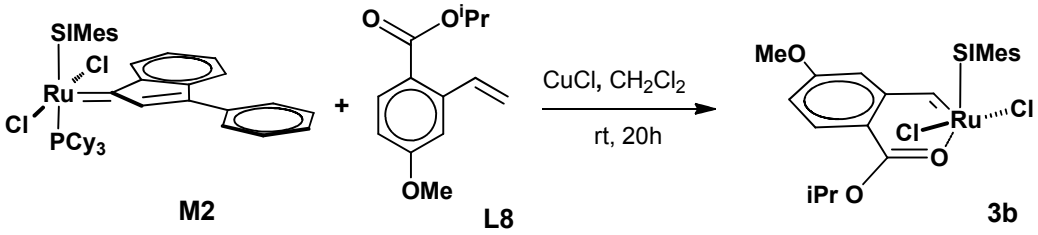

Figure 42. Procedure of the *trans*-complex **3b**

In a Schlenk flask, **M2** (91.8 mg; 0.0967 mmol; 1.0 eq.) was dissolved in degassed, dry CH_2Cl_2 (5 mL). 4-Methoxy-2-vinyl-benzoic acid i*so*-propylester (27.7 mg; 0.126 mmol; 1.3 eq.) and CuCl (9.6 mg, 0.0968 mmol, 1.0 eq.) were added. The reaction mixture was stirred under argon atmosphere for 21 h. The colour turned from deep red to deep green. The solvent was reduced to 1 to 2 mL and the *trans*-complex (**3b**) was separated from the *cis*-complex (**3a**) by column chromatography on silica gel using CH_2Cl_2/MeOH 20:1 (v:v) as eluent. Yields could not be determined, because inseparable by products were found in the product.

^{1}H-NMR (δ, 20°C, $CDCl_3$, 300 MHz): 18.79-18.44 (bs, 1H, Ru=CH), 8.00 (d, 1H, $^3J_{HH}$ = 8.7 Hz, ph^3), 7.10 (s, 4H, mes), 7.05 (dd, 1H, $^3J_{HH}$ = 8.8 Hz, $^4J_{HH}$ = 2.5 Hz, ph^4), 6.26 (d, 1H, $^4J_{HH}$ = 2.5 Hz, ph^6), 5.17 (m, 1H, $^3J_{HH}$ = 6.2 Hz, C*H*$(CH_3)_2$), 4.09 (s, 1H, H_2Im), 3.85 (s, 3H, OC*H*$_3$), 2.49, 2.40 (s, 18H, mes-C*H*$_3$), 1.25 (d, 6H, $^3J_{HH}$ = 6.1 Hz, CH(C*H*$_3)_2$. **Impurities**: *1-Methylene-3-phenyl-1H-indene:* 7.74-7.27 (m, aromats), 6.95 (s, C*H*$(C)_2$), 6.63 (s, C*H*$_2$=C), 5.80 (s, C*H*$_2$=C), *tricylclohexylphosphine:* 1.99-1.55 (m, Cy).

4.3.3. Cationic Ruthenium Complexes

4.3.3.1. [(SPY-5-34) - (Chloro) - (κ2(C,O)-(2-iso-propyl ester-5-methoxy benzylidene) - (pyridine)-(1,3-bis(2,4,6- trimethylphenyl)4,5-dihydroimidazol-2-ylidene)-ruthenium] chloride

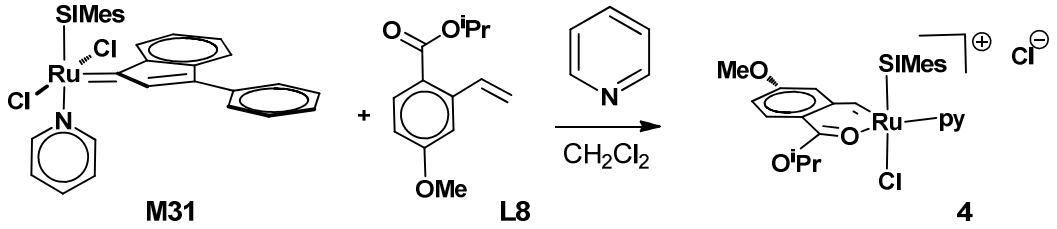

Figure 43. Reaction procedure of **4**

M31 (284.2 mg; 0.379 mmol; 1.0 eq.) was dissolved in 5 mL degassed CH_2Cl_2. 4-Methoxy-2-vinyl-benzoic acid-*iso*-propylester (99.7 mg; 0.453 mmol; 1.2 eq.) and pyridine (89.9 mg, 1.13 mmol, 3.0 eq.) were added. The reaction mixture was stirred in a Schlenk flask under argon atmosphere for 5 d, until the colour turned from deep red to deep green. After recording a NMR spectrum of the raw product (47% **3a** and 45% **4**), a purification step was set by column chromatography on silica gel using CH_2Cl_2/MeOH 5:1 (v:v). Yield: turquoise crystals (**4**, 106.7 mg, 37%), green-turquoise crystals were obtained as side product (**3a**, 78.1 mg, 29%).

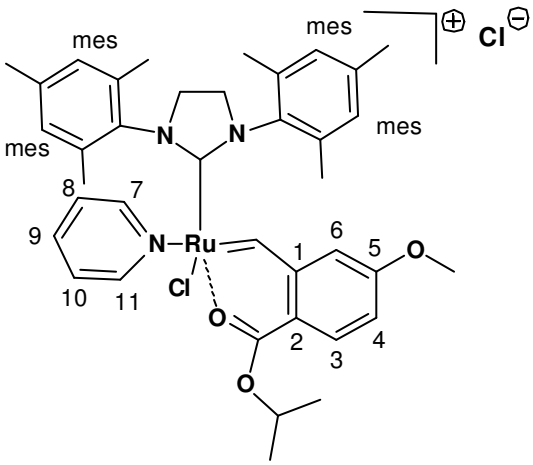

^{1}H-NMR (δ, 20°C, $CDCl_3$, 300 MHz): 17.93 (s, 1H, Ru=CH), 8.51 (d, 2H, $^3J_{HH}$ = 5.3 Hz, py^{7,11}), 8.04 (d, 1H, $^3J_{HH}$ = 8.8 Hz, ph^3), 7.75 (t, 1H, $^3J_{HH}$ = 7.2 Hz, py^9), 7.33 (t, 2H, $^3J_{HH}$ = 6.6 Hz, py^{8,10}), 7.31 (d, 1H, $^4J_{HH}$ = 2.1 Hz, ph^6), 7.20 (dd, 1H, $^3J_{HH}$ = 8.8 Hz, $^4J_{HH}$ = 2.1 Hz, ph^4), 7.07, 6.40 (s, 4H, mes), 5.29 (m, 1H, $^3J_{HH}$ = 6.2 Hz, $CH(CH_3)_2$), 4.17 (s, 4H, H_2Im), 4.01 (s, 3H, O*C*H_3), 2.66, 2.17, 1.64 (s, 18H, mes-CH_3), 1.57, 1.53 (d, 6H, $^3J_{HH}$ = 6.2 Hz, $CH(CH_3)_2$).

^{13}C-NMR (δ, 20°C, CD_2Cl_2, 75 MHz): 298.3 (1C, Ru=*C*H), 208.2 (1C, C_q, *C*NN), 175.4 (1C, C_q, *C*OO^{i}Pr), 166.1 (1C, C_q, ph^5), 155.2 (2C, py^{7,11}), 145.9 (1C, C_q, ph^1), 139.5, 136.6, 136.0 (6C, C_q, mes-*C*), 137.4 (1C, py^9), 133.6 (1C, ph^3), 133.4 (2C, C_q, mes-N), 130.4, 129.7 (4C, mes), 125.1 (2C, py^{8,10}), 115.7 (1C, ph^{4,6}), 114.5 (1C, C_q, ph^2), 113.3 (1C, ph^{3,4,6}), 73.6 (1C, *C*H(CH$_3$)$_2$), 56.7 (1C, O*C*H$_3$), 52.3 (2C, H_2Im), 21.9, 21.6 (2C, CH(*C*H$_3$)$_2$), 20.8, 18.2, 17.2 (6C, mes-*C*H$_3$).

4.3.3.2. [(SPY-5-34) - (Chloro)(κ^2(C,O)-(2-iso-propyl ester-5-methoxy benzylidene)(pyridine)(1,3-bis(2,4,6-trimethylphenyl)4,5-dihydroimidazol-2-ylidene)-ruthenium] hexafluoro phosphate

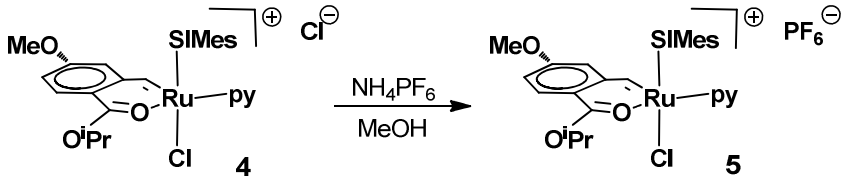

Figure 44. Preparation of complex **5**

In a Schlenk flask complex **4** (17.3 mg, 0.0226 mmol, 1.0 eq.) was dissolved in 2 mL degassed methanol under inert atmosphere. Ammonium hexafluorophosphate (8.8 mg, 0.0539 mmol, 1.1 eq.) was added. The reaction mixture was stirred at room temperature for 30 min. During this time a bluish precipitate formed, which was filtered, washed with methanol and eluated with dichloromethane. Yield: 12.9 mg (65%) blue crystals.

^{1}H-NMR (δ, 20°C, $CDCl_3$, 300 MHz): 17.87 (s, Ru=CH), 8.43 (d, 2H, $^3J_{HH}$ = 5.6 Hz, py^{5,9}), 8.04 (d, 1H, $^3J_{HH}$ = 8.8 Hz, ph^3), 7.72 (t, 1H, $^3J_{HH}$ = 7.5 Hz, py^7), 7.33 (bs, 1H, mes), 7.26 (t, 2H, $^3J_{HH}$ = 6.9 Hz, py^{6,8}), 7.20 (dd, 1H, $^3J_{HH}$ = 8.8 Hz, $^4J_{HH}$ = 2.5 Hz, ph^3), 7.12 (d, 1H, $^4J_{HH}$ = 2.5 Hz, ph^6), 6.84, 6.70, 6.00 (bs, 3H, mes), 5.30

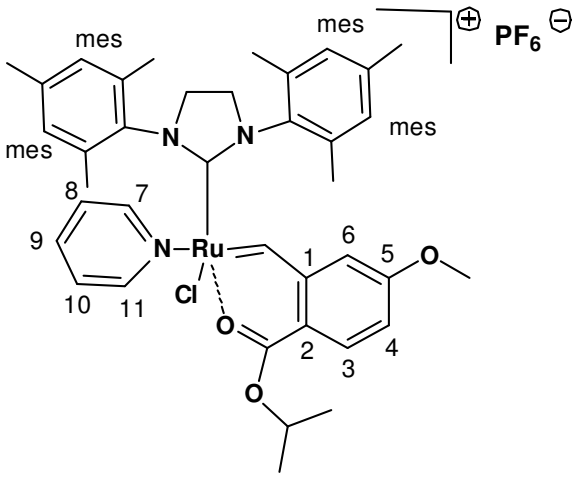

(m, 1H, $^3J_{HH}$ = 6.1 Hz, C*H*(CH_3)$_2$), 4.31-3.75 (bm, 4H, H_2Im), 3.99 (s, 3H, OC*H*$_3$), 2.82, 2.39, 1.95, 1.68, 1.52 (bs, 18H, mes-C*H*$_3$), 1.57, 1.53 (d, 6H, $^3J_{HH}$ = 6.1 Hz, CH(C*H*$_3$)$_2$).

^{1}H-NMR (δ, 20°C, CD_2Cl_2, 300 MHz): 17.70 (s, Ru=CH), 8.39 (d, 2H, $^3J_{HH}$ = 5.4 Hz, py^{5,9}), 8.12 (d, 1H, $^3J_{HH}$ = 8.8 Hz, ph^4), 7.80 (t, 1H, $^3J_{HH}$ = 7.6 Hz, py^7), 7.26 (t, 2H, $^3J_{HH}$ = 6.7 Hz, py^{6,8}), 7.26 (dd, 1H, $^3J_{HH}$ = 8.8 Hz, $^4J_{HH}$ = 2.8 Hz, ph^2), 7.96 (s, 1H, $^3J_{HH}$ = 2.5 Hz, ph^1), 7.08, 6.46 (bs, mes, 4H), 5.30 (m, 1H, $^3J_{HH}$ = 6.2 Hz, C*H*(CH_3)$_2$), 4.03 (bs, H_2Im, 4H), 3.95 (s, 3H, OC*H*$_3$), 2.57, 2.18, 1.53 (bs, 18H, mes-C*H*$_3$), 1.54, 1.52 (d, 6H, $^3J_{HH}$ = 7.0, 5.6 Hz, CH(C*H*$_3$)$_2$).

^{13}C-NMR (δ, 20°C, CD_2Cl_2, 75 MHz): Ru=CH not observed, 208.3 (1C, C_q, *C*NN), 175.3 (1C, C_q, *C*OO^{i}Pr), 166.0 (1C, C_q, ph^5), 154.7 (2C, py^{7,11}), 145.7 (1C, C_q, ph^1), 140.3, 137.3, 135.7 (6C, C_q, mes-*C*), 137.5 (1C, py^9), 133.8 (1C, ph^3), 133.5 (2C, mes-N), 129.7 (4C, mes), 124.9 (2C, py^{8,10}), 115.6 (1C, ph^{3,4,6}), 114.5 (1C, C_q, ph^2), 112.8 (1C, ph^{4,6}), 73.7 (1C, *C*H(CH_3)$_2$), 56.2 (1C, O*C*H$_3$), 51.6 (2C, H_2Im), 21.5, 21.3 (2C, CH(*C*H$_3$)$_2$), 20.6, 17.6, 16.7 (6C, mes-*C*H$_3$).

4.3.3.3. [(SPY-5-34) - (Chloro)(κ2(C,O)-(2-iso-propyl ester-5-methoxy benzylidene)(pyridine)(1,3-bis(2,4,6-trimethylphenyl)4,5-dihydroimidazol-2-ylidene)-ruthenium] hexafluoro phosphate

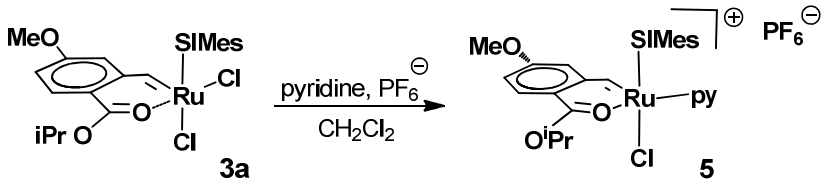

Figure 45. One-pot reaction procedure for **5**

For preparation of the cationic complex **5**, it was also tried to start from complex **3a**. Therefore, the Schlenk flask was charged with CH_2Cl_2 (2 mL), complex **3a** (50 mg, 0.0729 mmol, 1eq.) and pyridine (289 mg, 3.65 mmol, 50 eq.). The reaction mixture was stirred for 2 days at room temperature, then $NaPF_6$ (13.5 mg, 0.0804

mmol, 1.1 eq.) were added. Further, the mixture reacted for five more days. The raw product was purified by column chromatography, using CH_2Cl_2/MeOH, 20:1 - 5:1 (v:v). Three fractions were isolated, product **5** (as indicated by ^{1}H-NMR shift of 17.88 ppm) was found in small amounts in the ^{1}H-NMR spectrum of fraction 1, but it could not be isolated. (Further carbene containing products: 19.37 ppm (not identified), 17.92 ppm (**4**))

4.3.3.4. [(SPY-5-34) - (Chloro)(κ^2(C,O)-(2-methyl ester-benzylidene) (pyridine)(1,3-bis(2,4,6-trimethylphenyl)4,5-dihydroimidazol-2-ylidene)-ruthenium] hexafluoro phosphate

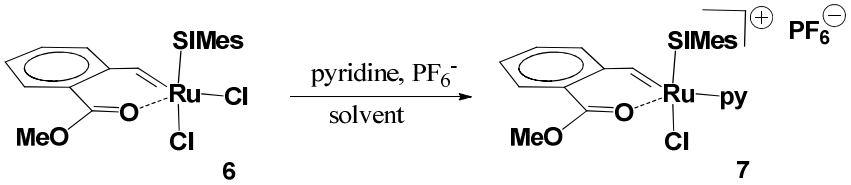

Figure 46. Typical procedure for formation of cationic pyridine complex **7**

For the preparation of **7** some experiments were carried out to find out, if there is a possibility to obtain the cationic PF_6^- complex, when starting from the *cis*-dichloro complex (**6**). Therefore, a solution of **6** (20 mg, 0.0319 mmol, 1 eq.), PF_6^- (1 eq.) and optional 10 eq. pyridine in 2 mL solvent (CH_2Cl_2, CH_3NO_2 or CHCN) was prepared and stirred at room temperature for a certain time. Reaction conditions and particular data can be found in Table 8 and Table 9. Conversions and isolated products were determined by ^{1}H-NMR spectrometry.

Table 7. Reaction conditions for Experiments 1-6

	reaction conditions
Experiment 1	1.0 eq. 6, 1.2 eq. $NaPF_6$, 10 eq. py, CH_2Cl_2, 18 h, rt
Experiment 2	1.0 eq. 6, 1.2 eq. $AgPF_6$, 10 eq. py., CH_2Cl_2, 14 h, rt
Experiment 3	1.0 eq. 6, 1.2 eq. $NaPF_6$, 10 eq. py., CH_3NO_2, 18 h, rt
Experiment 4	1.0 eq. 6, 1.4 eq. $NaPF_6$, CH_3NO_2, 2 h, rt
Experiment 5	1.0 eq. 6, 1.1 eq. NaPF6, CH_3CN, 2 h, rt
Experiment 6	1.0 eq. 6, 1.0 eq. $AgPF_6$, CH_3CN, 16 h, rt

Table 8. Carbene containing products (indicated by ^{1}H NMR, 300 Hz, $CDCl_3$) of Experiment 1-3 for one-pot synthesis of the cationic PF_6- complex (**7**).

	Experiment 1	**Experiment 2**	**Experiment 3**
before column	19.67 (62%) 19.49 (4%) 17.87 (34%)	19.68 (51%) 19.47 (7%) 17.87 (32%) further side products (10%): 18.84, 18.28, 17.61	19.48 (100%)
after column*	19.54 (94) 19.37 (6%) 17.85 (100%)	19.52 (93%) 19.37 (7%) 18.97 (11%) 18.73 (16%) 17.91 (48%) 17.57 (25%)	19.48 (100%)
after 6 days	19.32 (65%) 17.86 (35%) x	x	19.37 (78%) 17.86 (22%)

Table 9. Carbene containing products (indicated by ^{1}H NMR, 300 Hz, $CDCl_3$) of Experiment 4-6 for one-pot synthesis of the cationic PF_6- complex (**7**).

	Experiment 4	**Experiment 5**	**Experiment 6**
before column	19.03 (bs, 38%) 16.89 (11%) 17.85 (4%) further side products (47%): 19.30, 18.79, 18.56, 18.47	19.06 (bs, 80%) 17.83 (7%) 16.96 (6%) further side products (7%): 18.45	18.97 (bs, 48%) 16.94 (36%) further side products (16%): 19.30, 18.56, 18.49, 17.58
after column	19.66 (49%)* 17.86 (26%) 17.39 (9%) further side products (16%): 18.89, 18.45	19.03 (51%) 17.81 (12%) 16.96 (37%)	18.94 (57%) 16.93 (43%) 16.94 (100%)

*precipitate in $CDCl_3$

4.4. Ring Opening Metathesis Polymerization (ROMP)

4.4.1.1. Polymerization in Solution

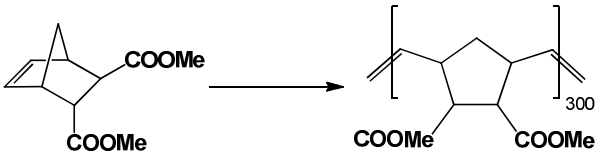

8 9

Figure 47. Typical polymerization procedure for monomer **8**

For a typical polymerization procedure a concentration of 0.1 M in respect to the monomer was used. In a Schlenk flask 1 eq. initiator was dissolved in the appropriate amount of degassed, dry dichloromethane. The mixture was heated to 40°C, then monomer **8** (300 eq.) was added. The reaction was followed by TLC using Cy/EtOAc, 3:1 (v:v) and $KMnO_4$ solution for staining. After complete conversion the reaction was quenched with an excess of ethyl vinylether and stirred for 15 minutes. Further, the solvent was evaporated to a volume of 2-3 mL and the polymer was precipitated in cold stirred methanol. The white solid was sampled and dried in vacuum. The same procedure was used for 80°C in toluene as the solvent.

4.4.1.2. Polymerization Procedure in NMR Tube (M:I = 70)

1 eq. initiator was weighted in a NMR tube and dissolved in 0.3 mL $CDCl_3$, the appropriate amount of monomer **8** (70 eq. in 0.4 mL $CDCl_3$) was injected. The propagation was monitored by ^{1}H-NMR (500 MHz) at 21,5°C, recording spectra every 10 minutes.

4.4.1.3. Polymerization Procedure in NMR Tube (M:I =5)

The NMR kinetic was prepared similar to the abovementioned procedure with 1 eq. initiator in 0.6 mL $CDCl_3$ and 5 eq. monomer **8** (dissolved in 0.3 mL $CDCl_3$). The polymerization's propagation was monitored by ^{1}H-NMR (300 MHz) at 21,5°C, recording spectra every few hours within the 8500 Hz region.

5. Appendix

5.1. List of Abbreviations

CuCl	copper chloride
Cy	cyclohexan
DFT	static density functional theory
dtbpm	bis(di-tert-butylphosphanyl)methane
EtOAc	ethyl acetate
GPC	gel permeation chromatography
H_2Im	4,5-dihydroimidazol-2-ylidene
k_i	initiation rate constant
k_p	propagation rate constant
M:I	monomer:initiator
M_n	number molecular weight
MWD	molecular weight distribution
NHC	N-heterocyclic carbene
NMR	nuclear magnetic resonance
PCy_3	Tricyclohexylphosphine
PDI	poly dispersity index
$Pd(PPh_3)_4$	Tetrakis(triphenylphosphine)palladium
py	pyridine
ROMP	ring opening metathesis polymerization
rt	room temperature
SIMes	saturated 1,3-dimesityl-imidazol-2-ylidene
SPY	square pyramidal
UV	ultra violet
TLC	thin layer chromatography
XRD	X-ray diffraction

5.2. List of Figures

5.3. List of Tables